



Effect of hot-melt extruded *Morus alba* leaves on intestinal microflora and epithelial cells

Hyun Bok Kim^a, Eun Ji Go^b, Jong-Suep Baek^{b,c,d,*}

^a National Institute of Agricultural Sciences, RDA, Wanju 55365, South Korea

^b Department of Bio-Health Convergence, Kangwon National University, Chuncheon 24341, South Korea

^c Department of Bio-Functional Materials, Kangwon National University, Samcheok 25949, South Korea

^d BeNatureBioLab, Chuncheon 24206, South Korea

ARTICLE INFO

Keywords:

Morus alba leaves
Hot-melt extrusion
Probiotics
Gut microbiota
Tight junction
Encapsulation

ABSTRACT

Although rutin and isoquercitrin have many effects, they are insoluble substances, making it difficult to obtain pure substances. This study was to investigate whether *Morus alba* leaves containing rutin and isoquercitrin could improve intestinal health by making a sustained-release formulation through a hot-melt extrusion (HME) process with improved stability and solubility and determine whether it could upregulate the balance of intestinal microorganisms and intestinal epithelial cells. A sustained-release formulation was prepared by the HME process using *Morus alba* leaves and a hydrophilic polymer matrix. Antibacterial activities of pathogenic microorganisms (*Escherichia coli*, *Streptococcus aureus*, *Enterococcus faecalis*) and proliferative effect of probiotics (*Lactobacillus rhamnosus*, *Pediococcus pentosaceus*) were tested against intestinal microorganisms. Regarding intestinal epithelial cells, a co-culture model of Caco-2 cells and RAW 264.7 cells was used. It was confirmed that the extrudate exhibited high antibacterial activities against pathogenic microorganisms and affected the proliferation of probiotics. Furthermore, after inducing inflammation through LPS, it recovered transepithelial electrical resistance-increased levels of tight junction proteins and decreased expression levels of pro-inflammatory cytokines. HME of *Morus alba* leaves containing rutin and isoquercitrin can upregulate intestinal microbial balance and intestinal epithelial cells.

1. Introduction

The major compounds present in *Morus alba* leaves are flavonoids, alkaloids, and phenolic acids [1]. The backbone of flavonoids is C6–C3–C3, which consists of two aromatic rings connected by a three-carbon ring. The primary flavonoids found in *Morus alba* leaves are isoquercitrin, quercetin, and rutin [2]. Two of these, isoquercitrin and rutin, are important antioxidant molecules [3]. Isoquercitrin has a high anti-inflammatory effect. However, it has an extremely low plant content, making it challenging to obtain enough in a pure state for the food and pharmaceutical industries [4]. Recently, many studies have been conducted to produce isoquercitrin from rutin [5]. The gastrointestinal tract and external environment can form biochemical and physical barriers that shield the mucosal membrane and peripheral organs from toxins and harmful bacteria [6]. The gastrointestinal tract (GIT), which is essential for human disease and health management, is home to a highly diverse gut microbiome [7]. Certain probiotics, such as *Lactobacillus rhamnosus* GG, can

* Corresponding author. Department of Bio-Functional Materials, Kangwon National University, Samcheok 25949, South Korea.
E-mail address: jsbaek@kangwon.ac.kr (J.-S. Baek).

improve intestinal epithelial cell function by modulating the expression of proteins including ZO-1 and occludin [8]. However, certain exogenous pathogens can change the makeup of the microbiome, interfere with the epithelial barrier, and result in certain infectious illnesses in the gastrointestinal tract.

With more than 1011 different types of gut microbiota, human GIT is a microbial ecosystem [7]. The development of immune cells, enteroendocrine function, and defense against pathogen overgrowth all depend on the gut microbiome [9]. To preserve homeostasis and avoid inflammation in the gastrointestinal tract (GIT), intestinal epithelial cells (IECs), which include paneth cells, absorptive epithelial cells, and goblet cells, form two different types of mucosal barriers that divide immune cells and gut microbes. Furthermore, by strengthening intestinal permeability and enhancing epithelial defense mechanisms, the gut microbiota can create a mucosal barrier [10]. To maintain gut homeostasis, interactions between the gut microbiome and IECs are essential. According to certain studies, tight junction regulation by the gut microbiota and IECs is a crucial regulator of epithelial permeability [11]. GIT homeostasis may also be orchestrated by the circadian clock and signals transduced by the gut microbiome [6].

The human immune system, nutrition processing, and energy homeostasis are just a few of the functions that are regulated by the hundreds of metabolites and proteins produced by the gut microbiota [12]. It has been determined that a few bacterial metabolites are crucial for controlling intestinal epithelial barrier integrity and IEC. For instance, the intestinal barrier depends on short-chain fatty acids (SCFAs), a class of metabolites produced when bacteria ferment dietary fiber. SCFAs control mucus production, luminal pH, and supply energy to epithelial cells [13]. To improve the function of the gut barrier and host metabolism, SCFAs can also control the differentiation and proliferation of IECs.

Enteroendocrine cells, Paneth cells, and absorptive enterocytes comprise the IEC monolayer [14]. IEC acts as a barrier between the microbiota in the stomach and the rest of the body. By releasing mucins, antimicrobial peptides, hormones, and type 2 immune mediators, various IEC subtypes can control the gut microbiome [15]. To separate the gut microbiota and IECs and prevent undesirable immune reactions, Paneth cells, for instance, can synthesize antimicrobial peptides and regenerate the islet-derived 3 family of proteins [16]. It has been reported that the production of serotonin by enterochromaffin cells regulates the composition of the gut microbiome [17]. Secretory vesicle differentiation may be aided by increased indoleamine 2,3-dioxygenase 1 expression in IECs [18]. Furthermore, a recent study discovered a novel function of IEC-derived liver kinase B1 (LKB1) in suppressing *Escherichia coli* microflora, which, by regulating IL-18 expression, may lessen susceptibility to colitis produced by dextran sulfate sodium (DSS) in a mouse model [18].

Intestinal nutrition, absorption, and development can all be significantly impacted by intestinal infections [19]. When a patient undergoes major surgery, severe burns, or hemorrhagic shock, the most frequent complication is infection [20]. Furthermore, intestinal infections caused by bacteria, viruses, or parasites can change the composition of the gut microbiome, cause tight junctions to break, and increase the permeability of the intestinal barrier [20]. In contrast, preventing pathogenic microbes from colonizing the body depends on the gut microbiome and IECs. It is unknown what mechanisms the gut microbiota use to provide colonization resistance (CR). Nonetheless, some research indicates that the gut microbiota may prevent the colonization of external microorganisms by promoting intestinal barrier integrity, bacteriophage deployment, competitive nutrient competition, and secretion of antimicrobial products [21]. To prevent pathogens from adhering abnormally, IECs can preserve the physical barrier function and release certain antibacterial compounds, mucus, and carbohydrates into the lumen [22]. Furthermore, the interaction between the gut microbiota and intestinal epithelial cells (IECs) during infection may be crucial in averting pathogen infection.

Isoquercetin and rutin are active components of *Morus alba* leaves. When applied to food development, the low water solubility of isoquercetin and rutin results in low bioavailability and absorption, although they have numerous biological activities [23]. Drug delivery systems (DDS) have long been used to treat insoluble drugs. By modifying the porosity, particle size, and wettability of poorly soluble drugs, solid dispersion (SD) technology is a popular formulation technique for improving drug solubility [24]. SD offers greater stability and a higher drug load than other nanoparticle systems. Spray drying, solvent evaporation, and HME are all included in SD [25]. For large-scale industries, HME is a solvent-free technology that works well [26]. Its benefits include continuous operation, high production efficiency, and online monitoring. Its process is straightforward and highly automated [27]. To achieve uniform drug dispersion in the carrier, it has a special blending geometry that induces high shear force and promotes mixing [28]. Because sustained-release formulations release the target drug gradually over time, they can minimize the number of drug administrations. Making a matrix with an insoluble polymer using solid dispersion formulation technology is an efficient way to create sustained-release oral dosage forms, among other formulation approaches for sustained drug release [29]. Drug molecules are evenly dispersed throughout the polymer matrix. A water-soluble or erodible matrix composed of different hydrophilic or hydrophobic polymeric excipients regulates drug release [30]. In the food industry, whey protein isolate (WPI) is becoming increasingly popular as a food biopolymer. WPI is desaturated by heat treatment above 60 °C, which reveals numerous hydrophobic functional groups on protein particle surfaces [31]. Lecithin is an amphiphilic surfactant that can bind to proteins through hydrophobic interactions, making it a natural emulsifier [32]. The solubility of the active ingredients can be increased using lecithin as a surfactant. It is also used as a plasticizer for matrices [33].

The purpose of this study was to see if a sustained-release formulation of HME-DDS employing *Morus alba* as a carrier might improve intestinal health by delivering continuous medication release to each location. To check the balance of intestinal microflora, its antimicrobial activities against harmful bacteria and its effect on the proliferation of probiotics were examined. To determine its intestinal epithelial cell recovery function, we determined whether it could promote high levels of transepithelial electrical resistance, anti-inflammatory activity, and tight junction-related gene expression. We also determined whether the HME-applied samples had the potential to enhance and maintain immunity in the intestinal environment or for use as prophylactic and therapeutic agents.

2. Materials and methods

2.1. Materials

S Food (Gumpo, Korea) provided the whey protein isolate, lecithin, and ascorbyl palmitate used in the extrudates. The source of the citric acid was Daejung (Sihung, Korea). We purchased isoquercitrin, rutin, quercetin, and caffeic acid from Sigma-Aldrich (St. Louis, MO, USA). Potassium acetate and aluminum chloride hexahydrate were acquired from Junsei Chemical (Tokyo, Japan). The American Type Culture Collection (ATCC) provided the following microorganisms: *Lactocaseibacillus rhamnosus* (*L. rhamnosus*), *Escherichia coli* (*E. coli*), *Streptococcus aureus* (*S. aureus*), and *Enterococcus faecalis* (*E. faecalis*). Brain heart infusion (BHI) and Man-Rogasa-Shape (MRS) were acquired from Solarbio (Shanghai, China).

2.2. Development of colloidal solid dispersion systems by HME

HME applied MAL with a twin-screw extruder and a die (1 mm) at an injection speed of 40 g/min and 150 rpm. It was carried out at a temperature of 70–100 °C. After that, a freeze-dryer was used to dry the extrudate. A lyophilized sample was then obtained in powder form through a grinder. Table 1 shows formulation compositions.

2.3. Total flavonoid and phenol content analysis

We calculated the total flavonoid content in accordance with Do et al. [34,34]. A published procedure was used to carry it out [21]. The reaction was then allowed to sit in the dark for 30 min after 0.1 mL of 10 % aluminum chloride hexahydrate and 1 M potassium acetate were added to the extract. At 415 nm, absorbance was measured with a spectrophotometer. To create a standard curve, quercetin and gallic acid were used as reference materials. The amount of total phenol was calculated in accordance with Lim et al. [35]. In summary, the sample (200 µL), 1 mL of FolinDenis, and 0.8 mL of sodium carbonate were combined and left to incubate for 45 min in the dark. At 760 nm, absorbance was measured with a spectrophotometer. Gallic acid was used as a reference material to create a standard curve.

2.4. High-pressure liquid chromatography (HPLC) analysis

Agilent Technologies 1200 series was used for HPLC quantification. ODS-AM C18 was employed in the column. Standard materials included rutin and isoquercitrin. The parameters that were employed were as follows: 1.0 mL/min flow rate; 10 µL injection volume; 35 °C oven temperature; 356 nm detector wavelength; gradient mobile phase; solvents A and B, acetonitrile and water; elution times (min), 0 min with 82 % A and 18 % B; 9 min with 62 % A and 35 % B; 11 min with 82 % A and 18 % B, and 22 min with 82 % A and 18 % B.

2.5. Polydispersity index (PDI) and particle size measurements

Using Katsuhiro's analysis method, DLS (Zetasizer Nano ZS, Malvern Instruments, Malvern, UK) measured the size, zeta potential, and polydispersity index (PDI) of the produced HME-DDS sample's particles [36]. To get ready for the DLS measurement, samples were spread out in distilled water.

2.6. Examination of fourier-Transform infrared spectroscopy (FT-IR)

In the same way that Chaitanya did, to verify the molecular structure, FT-IR (FT-IR spectrophotometer and Microscope) was employed. E [37]. By using FT-IR measurements, the formation of chemical bonds or entities was verified.

2.7. Analysis of transmission electron microscopy (TEM) with scanning electron microscopy (SEM)

Huseynov's method was used to temporally confirm the particle morphology of each sample using SEM and TEM [38]. To verify the

Table 1
Formulation ratio of *Morus alba* leaf and biopolymers (%).

	MAL-HME-F1	MAL-HME-F2	MAL-HME-F3
<i>Morus alba</i> leaf powder	79	69	49
Whey protein isolate	10	20	40
Lecithin	2.5	2.5	2.5
Vitamin C	2	2	2
Vitamin E 50 %	2	2	2
Citric acid	2	2	2
Ascorbyl palmitate	2	2.5	2.5
Total	100	100	100

morphology with unaided eyes, platinum-coated samples were examined using a field emissions scanning electron microscope and observed at a voltage of 5 kV. The sample was dispersed in methanol and dried on filter paper (1002-090, 90 mm, Whatman, Maidstone, UK) in order to visually check transmittance of the sample with a TEM. To visually verify each sample's transmittance, the image was examined.

2.8. Research on *In vitro* release

The approach outlined by Jin et al. [39] was used to conduct the release studies. To maintain the sink total volume, 2 mL of the release solution was removed for testing at 0.5, 1, 2, 4, 8, 12, and 24 h and replaced with an equal amount of fresh medium.

2.9. Bacterial strains and growth conditions

L. rhamnosus and *P. pentosaceus* were probiotic bacterial strains used in this study. They were cultured with MRS liquid or MRS agar at 37 °C. *S. aureus*, *E. coli*, and *E. faecalis* were pathogenic bacteria used in this study. They were cultured with BHI liquid or BHI agar at 37 °C.

2.10. Measurement of antibacterial activity against pathogenic bacteria

The concentration of each pathogen inoculated into the BHI broth was fixed at 10^8 CFU/mL. OD600 values were ascertained using UV/VIS after extracts of HME-MAL-F2 or unextruded MAL were added in concentrations between 1 and 6 mg/mL. They were incubated at 37 °C for 24 h. Growth monitoring of pathogenic bacteria was performed over time. Inoculation of pathogenic bacteria without MAL was used as a control.

2.11. Effects of *Morus alba* leaves on proliferation of probiotics

To confirm effect of the HME-MAL-F2 formulation on growth of *L. rhamnosus* and *P. pentosaceus* probiotics, the degree of proliferation was evaluated by flat colony counting [36]. The non-extruded product (MAL) and HME-MAL-F2 were prepared to a final concentration of 2 mg/mL. It was then mixed with 50 μ L of probiotics to achieve a final cell density of 10^7 CFU/100 μ L. MAL and HME-MAL-F2 samples were mixed and grown on MRS agar medium for 24 h at 37 °C. Numbers of colonies formed after 24 h of culturing the two types of probiotics on MRS agar were counted. Cultured probiotics were used as controls without sample treatment.

2.12. Formulation on pH change of probiotics culture medium

After 1 mL of the probiotic solution (10^7 CFU/mL) was inoculated into a new MRS (100 mL), HME-MAL-F2 and MAL samples were then added. The strain suspension was detected after 24 h of incubation at 37 °C. A pH meter was also used to take readings every 4 h.

2.13. Release properties of additional *Morus alba* leaves regarding growth of probiotic strains

In this process, the same method used for pH change analysis was used for probiotic culture and sample processing. Each sample was examined. Following co-culture, samples (3 mL each) were removed for HPLC analysis every 4 h and replaced with the same volume of fresh media to maintain the sink. Contents of rutin and isoquercitrin contained in HPLC samples were determined using MAL and HME-MAL-F2 samples obtained at each hour for determining the cumulative release rate for each hour. Release rates of rutin and isoquercitrin amounts in relative proportions were calculated.

2.14. Effects of *Morus alba* leaves on antibacterial activities of probiotics

Antibacterial activity was determined with the paper disk diffusion method after additional treatment with HME-MAL-F2 of MAL and probiotic monocultures, *L. rhamnosus* and *P. pentosaceus*. Pathogenic microorganisms (*S. aureus*, *E. faecalis*, *E. coli*) with a final concentration of 10^6 CFU/100 μ L were plated on BHI solid medium. The inner diameter of the plated bacterial medium was 10 mm. 100 μ L of *L. rhamnosus* and *P. pentosaceus* was prepared, representing a final concentration of 10^7 CFU/100 μ L. After punching 4 round wells, *L. rhamnosus* and *P. pentosaceus* cell suspension were mixed and used for treatment. Samples were treated with pathogens spread onto a Petri dish and incubated at 37 °C. To evaluate antibacterial activity, the diameter (clear zone, mm) of the growth inhibition zone formed around each well after 24 h was measured.

2.15. Cell culture conditions

Effect of HME-MAL-F2 on tight junction of human small intestine, Caco-2 cells was placed in the apical compartment. After a semi-permeable membrane was placed, RAW 264.7 macrophage was constructed and co-cultured in the basolateral compartment to determine the effect of pharmacological components. An *in vitro* gut inflammation model was constructed to investigate effects on transport, metabolism, and cell-cell interactions. Korean Cell Line Bank (KCLB, Seoul, Korea) provided Caco-2 cells (30037.1) and RAW 264.7 macrophages (40071). For cell culture, Gibco (Grand Island, NY, USA) provided DMEM, PBS, penicillin-streptomycin

solution, and 0.05 % Trypsin-EDTA solution, as well as (FBS), and 30-mm cell culture dishes were used. Caco-2 cells were grown in DMEM media with 10 % FBS and 1 % antibiotics. Cells were cultivated in an incubator with 5 % CO₂ at 37 °C.

2.16. Toxicity evaluation through MTT assay

Toxic effects of MAL and HME-MAL-F2 samples on cell stimulation and viability were evaluated using MTT assays. Briefly, RAW 264.7 cells (Passage: 28) at 4×10^4 cells/well and Caco-2 cells (Passage: 36) at 5×10^4 cell/well were seeded into 96-well plates (32096, SPL life sciences, Pochon, Korea). After seeding, cytotoxicity test was performed when cells reached 80 % confluency. After culturing cells in 24-well plates to 80 % confluent, samples were diluted to different concentrations (1, 2, and 4 mg/mL, including 2 mg/mL which showed the effect of inhibiting pathogen activity and probiotics proliferation) in the culture medium and used for pre-treatment for an hour. After 24 h of sample treatment, a well was filled with 10 L of MTT solution and incubated for 4 h at 37 °C. 200 μ L of DMSO was added to stop the reaction after the supernatant was removed. The purple formazan was completely dissolved by shaking the plate sufficiently while blocking light. Following the administration of 50 μ L of each onto a 96-well plate, the cytotoxicity was assessed by employing a microplate reader (US/Epoch, USA) to measure absorbance at 570 nm. The measured absorbance was substituted into the formula below to calculate cell viability.

$$\text{Cell viability (\%)} = \frac{A_{\text{treatment}} - A_{\text{blank}}}{A_{\text{control}} - A_{\text{blank}}} \times 100$$

2.17. Implementation of an in vitro intestinal inflammation model

Caco-2 cells (Passage: 36) were inoculated as an apical compartment in a 6 trans well insert plate at 1×10^5 cells/well at 2 mL each. For Caco-2 cells, the medium was replaced by 2 mL every 2–3 days for 21 days. At the time of medium exchange, the existing culture medium was carefully removed so as not to impact the membrane and a new culture medium was added to the apical compartment. RAW 264.7 cells (Passage: 28) were inoculated into the basolateral compartment in a 6-well plate with 1×10^5 cells per well (3 mL each) and cultured for 48 h for cell attachment. After cell culture was complete, the 6-trans well insert plate in which Caco-2 cells were cultured was transferred to a 6-well plate (30006, SPL life sciences, Pochon, Korea) in which RAW 264.7 cells were cultured. Then all media were replaced with serum-free DMEM media. When Caco-2 cells used in the experiment were cultured for 2–3 weeks, a cell monolayer of integrity combined with tight junction proteins was formed. When the monolayer of Caco-2 cells was formed, the transepithelial electrical resistance (TEER) value was $800 \Omega \times \text{cm}^2$ or more [40]. When samples and LPS were used for treatment, the TEER value was $800 \Omega \times \text{cm}^2$ or higher, indicating that the Caco-2 cells cultured on the Transwell plate formed tight junctions. After 2 mg/mL samples of MAL and HME-MAL-F2 were diluted with serum-free DMEM medium and used to treat Caco-2 cells cultured in apical wells for 24 h, basolateral wells were washed twice with PBS and 2 μ g/mL of LPS (lipopolysaccharides from *Escherichia coli* O111:B4, L3012-5 MG, Sigma-Aldrich Co., St. Louis, MA, USA) was added to serum-free DMEM medium.

2.18. Measurement of transepithelial electrical resistance

To determine effects of MAL and HME-MAL-F2 samples on tight junction integrity of Caco-2 cells, transepithelial electrical resistance (TEER) was measured. For TEER measurement, a Millicell ERS-2 resistance meter (Millipore, Burlington, MA, USA) was used. The long side of the probe was perpendicular to the bottom surface of the basolateral well and the short side was slightly immersed in the medium of the apical well to measure TEER. Before moving from the measured well to the next well, it was measured after lightly washing with PBS. The TEER value was measured in three repetitions. It was calculated as follows by referring to the user manual of the machine using the following formula: TEER (transepithelial electrical resistance) = resistance (Ω) \times membrane area (cm^2).

2.19. Cytokine measurement in the apical compartment

The increase in permeability between cells due to decreased function of tight junctions following LPS treatment and the resulting transfer of inflammatory cytokines from RAW 264.7 cells from the basolateral compartment to the apical compartment were measured. Levels of NO (EMSNO), IL-1 β (BMS600-2), PGE₂ (KHL1701), and TNF- α (BMS607-3) among cytokines were measured using an Invitrogen ELISA kit (Waltham, MA, USA). Cytokine content in the apical compartment was analyzed where Caco-2 cells were present.

2.20. Total RNA isolation

To determine expression of tight junction-related genes at mRNA level, Caco-2 cells were treated with MAL and HME-MAL-F2 samples for 24 h. Caco-2 cells when then treated with LPS for 24 h and 2 mL of PBS and stored at 4 °C. Following two rounds of washing, Caco-2 cells were isolated from each well, and a Hybrid-R kit (305-101, GeneAll, Seoul, Korea) was utilized to extract total RNA. Extracted RNA was dissolved in DEPC-H₂O, and RNA concentration was measured at 260/280 nm using a Nano Drop Spectrophotometer. A260/A280 ratio of 1.8–2.1 RNA was employed. Total RNA was isolated and kept at –70 °C.

2.21. Reverse transcription reaction

Reverse transcription (RT) was used to create cDNA from isolated total RNA. The reverse transcriptase used in the experiment was Hyperscript 2X RT Master mix (601–710, GeneAll, Seoul, Korea). The total reaction solution was 20 μ L. It was prepared by adding 10 μ L of master mix, 1 μ L of oligo dT, total RNA, and RNase-waterWith Applied Biosystems' Simpli Amp Thermal Cycler (Waltham, Massachusetts, USA), Reverse transcription was carried out at 55 $^{\circ}$ C for 60 min, reverse transcription inactivation at 95 $^{\circ}$ C for 5 min, and priming at 42 $^{\circ}$ C for 5 min in order to synthesis cDNA. The cDNA that was generated was kept at 4 $^{\circ}$ C.

2.22. Quantitative RT-PCR (qRT-PCR) analysis

The synthesized cDNA was used in quantitative RT-PCR experiments to determine the expression level of gene of interest. The instrument used in this experiment was a Light Cycler 96 system (788BR06094, Bio-Rad, Hercules, CA, USA). Primers used for the gene of interest (Bioneer Inc., Daejeon, Korea) had a GC content of 45 %. It was designed to be -64 %. The total volume was set to 20 μ L. Which included 10 μ L PCR matrix mix (24367659, GeneAll, Seoul, Korea), 0.5 μ L (50 pmole) forward primer, 0.5 μ L (50 pmole) reverse primer, cDNA (2 μ g/ μ L), and distilled water (DW). Real-time PCR was performed using the Universal Probe Library method in the Light Cycler 96 system PCR system and β -actin was used as a housekeeping gene (Table 2). PCR reacts first at 95 $^{\circ}$ C, 10 minutes (initial denaturation), then 40 times at 95 $^{\circ}$ C, 15 s (denaturation), 55 $^{\circ}$ C, 30 s (annealing), and 72 $^{\circ}$ C, 30 s (extension). Table 2 shows the base sequences of primers used in PCR.

2.23. Statistical analysis

All statistics were analyzed using SPSS. Statistical significance was set at $p < 0.05$ level. Between-group analysis was performed through One-way ANOVA (Analysis of variance). Results were validated by Tukey's range test.

3. Results and discussion

3.1. Total phenolic contents

When comparing MAL and HME-MAL, it was found that contents of flavonoid, phenol, rutin, and isoquercitrin were increased in HME-MAL than in MAL (Table 3). This finding is in line with a prior study that demonstrated that the solid shear force used during the extrusion process increased the extraction efficiency [41]. This was also consistent with another study that found that mechanically reducing the particle size increased bioavailability [42]. Additionally, it was found that HME-MAL-F1, -F2, and -F3, in which excipients were treated by concentration, showed higher contents. It has been reported that whey protein isolates and lecithin used as excipients can improve solubility and stability of bioactive compounds [43]. Whey protein might provide better encapsulation and protection for nutraceuticals than other materials because of its flexible shape and increased hydrophobic segments exposed to the outside by heat treatment [44]. Due to these significant factors, WP has been widely studied for drug delivery purposes so far [45]. It is preserved until it is released from a specific target site in the body through the functional group of the polypeptide structure [46]. It was confirmed that the bioactive component of the bioactive compound could be increased by the HME extrusion process, such as an excipient [47]. Therefore, it was confirmed that the HME process could lead to a high extraction yield.

3.2. Particle size and size distributions

Particle size and size distribution are critical parameters used to evaluate the physical stability of nanoparticles. When the particle size was compared, it was found that particle sizes of HME-MAL-F1, -F2, and -F3 after adding the excipient and the HME process were

Table 2
Sequences of sense and antisense primer applied to reverse transcriptase-quantitative PCR (RT-qPCR).

Gene	Orientation	Primer sequence (5' \rightarrow 3')
ZO-1	sense	AAATTTAACTAATGTCAGACTGGAGGA
	antisense	TCAGCTTGTTGGTAGTAAGAGG
occludin	sense	AAGGGAGCCTGTCTATTGGAA
	antisense	AAAAAGCATGCAACTTGAAGA
JAM-1	sense	CAGCTCCTGTGGGGAAAG
	antisense	TGCTCTTCAGAACGAGTCACC
claudin-1	sense	CACCGTCTGTGTTGAGCA
	antisense	CAAACCACCGCTTACAGATG
claudin-3	sense	AACCTGCATGGACTGTGAAA
	antisense	GGTCAAGTATTGGCGGTAC
claudin-4	sense	AACCTGTCCCCGAGAGAGA
	antisense	GCAAGTGTGAGCAGACCAGT
β -actin	sense	AAGTCCCTTGCCATCCTAAA
	antisense	ATGCTATCACCTCCCCTGTG

Table 3

Total phenolic and total flavonoid contents (mg/g).

	Total phenol contents (mg/g)	Total flavonoid contents (mg/g)	Rutin ($\mu\text{g/g}$)	Isoquercitrin ($\mu\text{g/g}$)
MAL	9.71 ± 0.88^a	1.70 ± 0.26^a	54.61 ± 2.19^d	1.66 ± 0.18^d
HME-MAL	8.04 ± 0.26^b	2.19 ± 0.25^a	501.95 ± 9.39^c	127.95 ± 2.50^c
HME-MAL-F1	10.03 ± 1.09^a	2.71 ± 0.05^a	1143.47 ± 4.41^a	238.09 ± 5.76^a
HME-MAL-F2	10.27 ± 1.04^a	2.57 ± 0.38^a	972.17 ± 25.92^b	197.50 ± 5.18^b
HME-MAL-F3	10.41 ± 0.22^a	1.84 ± 0.64^a	1004.82 ± 36.66^b	223.12 ± 7.10^a

reduced to 300 nm or less. Lee et al. [42] have reported that HME could reduce particle size (Table 4). PDI represents the average particle size and size distribution. A PDI value between 0.1 and 0.5 indicates a typical size distribution [48]. It was confirmed that PDI values of all samples were within the typical range. Particles with an absolute zeta potential value of less than 30 generally indicate good stability [48]. The zeta potential of the extrudate sample was low, indicating that particles were stable.

3.3. FT-IR spectroscopy

FT-IR showed various functional groups of biomolecules adsorbed on the particle surface and indicated the formation and stabilization of a formulation according to the decrease and increase of an organic matter [49] (Fig. 1). Peaks at 1020 cm^{-1} (C–H deformation of aromatic ring) [50], 1371 cm^{-1} (C–H bending band) [51], 1605 cm^{-1} , and 1700 cm^{-1} represented stretching vibrations of the carboxyl group [52]. The peak at 2918 cm^{-1} represented a C–H stretching vibrational group in methylene [52], indicating that the environment was less lipophilic due to induced fragmentation of lipoproteins [53]. The peak at 3289 cm^{-1} represented a phenolic or alcohol band [54] that might play a role in OH stretching and stabilization, suggesting that it might have been derived from OH groups of carbohydrate proteins and polyphenols [55].

3.4. Morphology of particle

Images obtained using SEM can show surface properties of powder particles, including particle size and distribution, shape, and texture. The morphology was visualized at 1,000x. Raw *Morus alba* leaves were observed to have rough particles. Extrudates without the addition of excipients had relatively less rough spherical particles (Fig. 2A and E). It could be seen that lecithin, an excipient added to F1, F2, and F3 extrudates, protected the shape of particles [56]. And the HME processed extrudate had a smooth surface and reduced particle size (Fig. 2B–D). The HME process as a method for producing amorphous materials has been reported [56]. Since proper excipient selection and application of HME can significantly increase the intensity of diffraction peaks of *Morus alba* leaves, they can have an amorphous form [57]. Amorphous grains allow increased crystallite segregation to relieve incoherent stresses and allow non-catastrophic nano-cracking along grain boundaries [58]. It was observed that the particle size of extruded leaves was reduced compared to that of raw *Morus alba* leaves, consistent with a previous reported showing that the extrudate obtained by HME could show particle size reduction and uniformity [59]. Additionally, stability of the component might have been increased due to particle size reduction [60]. Results of SEM could support results of PSA, PDI, and ZP visualized in TEM images. Raw *Morus alba* leaf image was consistent with the average particle size measurement result (Fig. 3A). Particles of the *Morus alba* leaf extrudate were relatively reduced with a uniform spherical shape and a diameter of less than 500 nm (Fig. 3B). The region rich in components scattered electrons more. It might appear as a dark part contrasting with a bright part [61].

3.5. In vitro release

HME processing is a method that can increase the usage of ingredients by dispersing active ingredients in a polymer matrix. It has been proven that HME formulations can effectively improve the bioavailability and drug delivery of poorly soluble drugs [62]. Emission profiles of the raw sample without HME and the sample with HME were obtained (Fig. 4). In particular, the cumulative release rate of the HME-MAL-F2 formulation was significantly increased compared to that of the original sample (MAL) (Fig. 4A, G). In the case of the virgin sample, HME decreased particle size and accelerated component release due to the increased surface area. Additionally, the matrix of particles was changed after the HME. The structure of the raw sample was changed due to physical treatment (pressure, heat) so that a tremendous amount of ingredients could be used in the extrusion formulation [63]. Samples of extrudates showed sustained release characteristics compared to *in vitro* release results of rutin [63]. Sustained release means that the

Table 4Particle size, PDI, and Zeta potential of *Morus alba* leaves.

	PSA (nm)	PDI (index)	ZP (mV)
MAL	2273.57 ± 498.24^b	0.306 ± 0.02^b	-24.033 ± 0.924^a
HME-MAL	4384.37 ± 943.12^a	0.380 ± 0.03^a	-33.733 ± 1.222^d
HME-MAL-F1	166.57 ± 4.91^c	0.227 ± 0.01^c	-29.6 ± 0.361^c
HME-MAL-F2	292.43 ± 204.73^c	0.225 ± 0.04^c	-25.833 ± 1.266^b
HME-MAL-F3	141.1 ± 20.26^c	0.250 ± 0.02^c	-26.267 ± 0.802^b

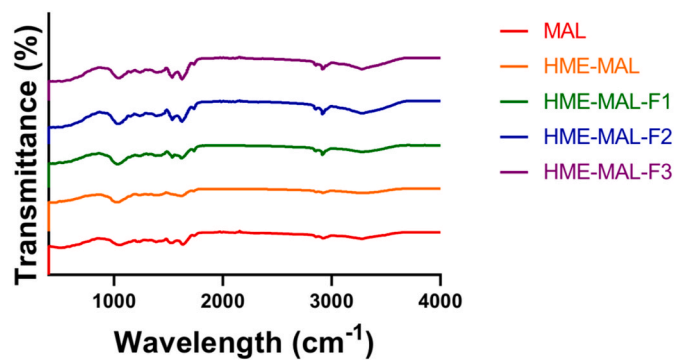


Fig. 1. FT-IR study of the solid formulation of *Morus alba* leaf extrudate prepared with various chemical additions.

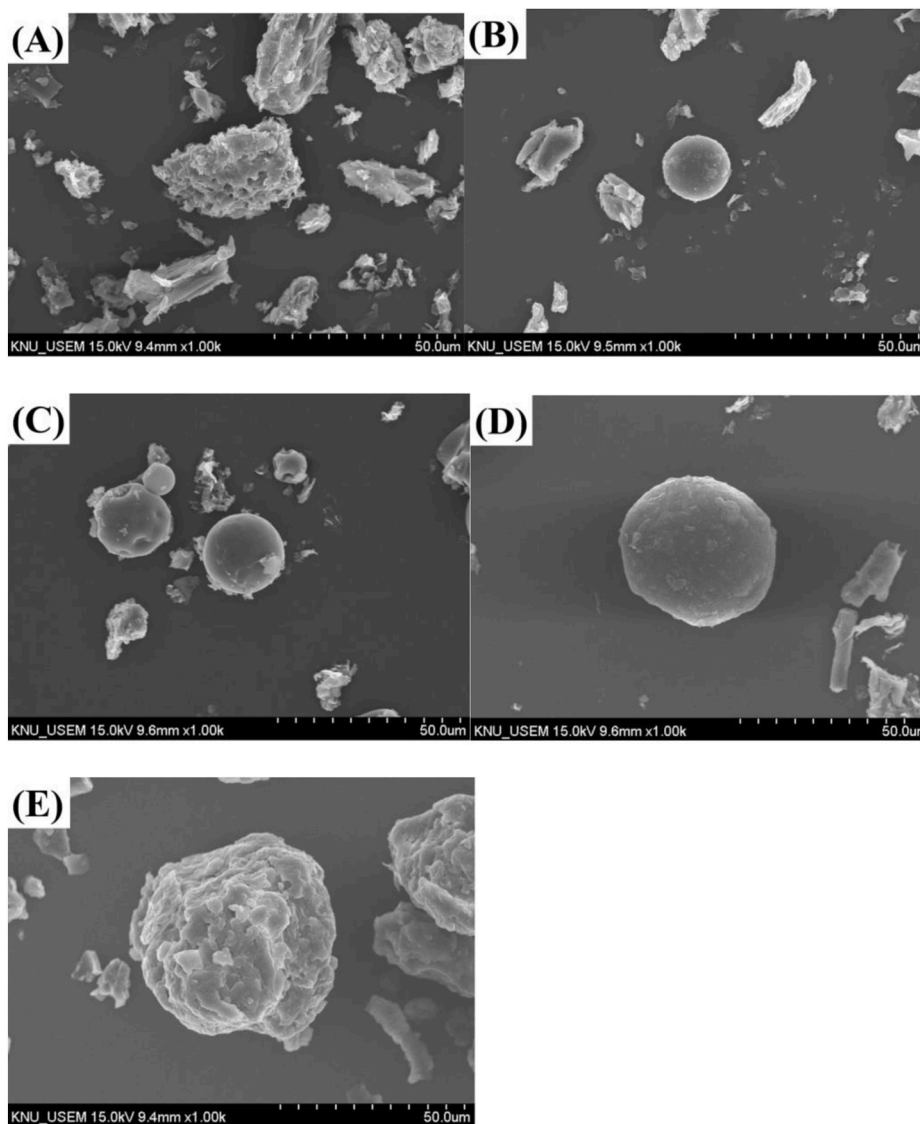


Fig. 2. Scanning electron microscopy images of non-extrusion and *Morus alba* leaf extrusion. (A) *Morus alba* leaf, (B) HME-MAL-F1, (C) HME-MAL-F2, (D) HME-MAL-F3, (E) HME-MAL.

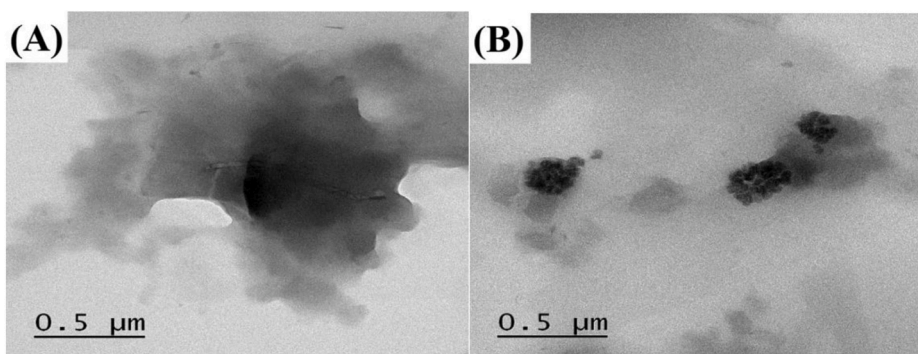


Fig. 3. Transmission electron microscopy images of non-extrusion and HME-MAL-F2. (A) MAL, (B) HME-MAL-F2.

drug is released continuously. This means that the therapeutic effect time of the drug is prolonged (Fig. 4A, B, C, D), with the number of administrations reduced compared to other agents. In addition, its biocompatibility can be increased (Fig. 4E, F, G, H).

3.6. Minimal inhibitory concentration of formulation

MIC was determined to select the minimum concentration at which the sample could inhibit bacteria to minimize bacteria. It was confirmed that MAL and HME-MAL-F2 could inhibit pathogenic bacteria such as *E. coli*, *E. faecalis*, and *S. aureus* (Fig. 5). As a result, it was found that the growth of bacteria was inhibited when MAL was used for treatment at 5 mg/mL for *E. coli* and *S. aureus* and at 7 mg/mL for *E. faecalis* (Fig. 5A, C, E). On the other hand, it was confirmed that *E. faecalis* and *S. aureus* were inhibited by HME-MAL-F2 at a concentration of 2 mg/mL and that *E. coli* was inhibited by HME-MAL-F2 at a concentration of 1 mg/mL (Fig. 5B, D, F). The difference in MIC value from those in other papers might be due to the use of water extract rather than ethanol extract in the present study. It is known that differences in actual MIC values can be attributed to chemical compounds, extraction methods, concentrations of bioactive compounds, and selected bacterial strains [64]. Furthermore, *Morus alba* leaves can alter transepithelial ion transport [65]. Trans-epithelial ion transport is involved in the integrative function of the gastrointestinal tract, which acts as a barrier to protect against pathogenic microorganisms [66]. It has been reported that flavonoids of *Morus alba* leaves can inhibit the growth of three pathogenic microorganisms [67]. MAL also inhibited the growth of pathogenic microorganisms in the present study. However, the extrudate exhibited a high inhibitory activity. This is because flavonoids and their metabolites can permeate bacterial cells and a large amount of matrix material inside bacterial cells will leak out, resulting in an antibacterial effect [68].

3.7. Effects of sterilized MAL and HME-mal-f2 on growth of probiotics

Probiotics can regulate the microbiome and immune system by inhibiting the growth of pathogenic microorganisms [69]. *Lactobacillus* and *Pediococcus* are the most used probiotics [70]. *L. rhamnosus* [71]. And *P. pentosaceus* [72] are widely located in the human body and increase the production of fatty acids in the intestine. It maintains intestinal homeostasis and plays a key role in human health, including inflammatory bowel disease.

L. rhamnosus and *P. pentosaceus* were concurrently treated with samples and examined by flat colony counting to determine the effects of MAL and HME-MAL-F2 on probiotic growth [73]. It was found that the number of colonies increased after MAL and HME-MAL-F2 treatment (Fig. 6A and B). Rutin and isoquercitrin in *Morus alba* leaves have been proven to be helpful for the balance of intestinal microorganisms. A study [74] has found that rutin and isoquercitrin can promote cell growth of lactic acid bacteria, such as those present in the intestinal microflora. Additionally, it has been reported that intestinal microflora can be regulated by the HME extrusion process [75]. In the case of Con, where *L. rhamnosus* was cultured at a level of 10^7 CFU/mL without sample treatment, the number of colonies was $91.67 \pm 25.00 \times 10^9$ CFU/mL (Fig. 6C). In *L. rhamnosus* treated with MAL, the number of colonies was more than 2.5 times higher than in Con. In the case of HME-MAL-F2, it was confirmed that the number of colonies was more than five times higher than that of Con, showing a proliferation effect. Furthermore, it was confirmed that *P. pentosaceus* cells proliferated in the same order as Con < MAL < HME-MAL-F2. These results suggest that MAL-HME-F2 can regulate microbial flora by contributing to the growth of lactic acid bacteria.

3.8. pH changes of probiotics culture medium

MAL and HME-MAL-F2 were co-cultured with lactic acid bacteria and pH changes over time were monitored. A decrease in pH during the culture of lactic acid bacteria indicates the production of organic acids containing phenolic acids and short-chain fatty acids [76]. Flavonoids are involved in many interactions between gut microbes. They can exert a selective proliferative effect on intestinal microorganisms and become degraded [77]. In addition, aglycones can be released from flavonoid glycosides. Improving the biochemical environment for microbial growth is one of the probiotic mechanisms of phenolics [78]. Flavonoids contain phenolic hydroxyl groups to lower the pH of culture [79]. It was confirmed that when MAL and HME-MAL-F2 were co-cultured, the pH was

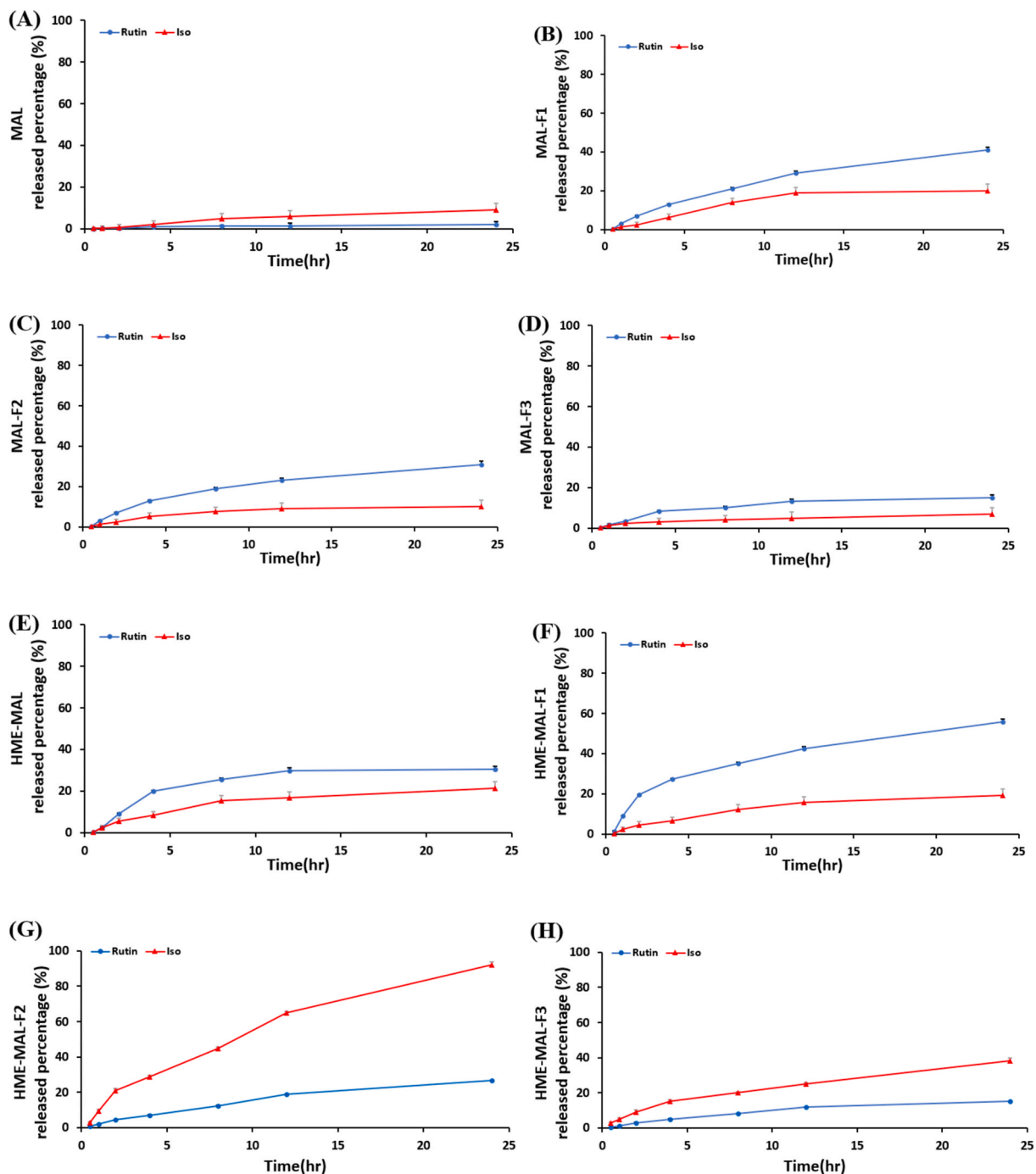


Fig. 4. Release profiles of rutin, isoquercetin from *Morus alba* leaf and HME-MAL-F1, F2, F3 in gastrointestinal tract simulation. (A): MAL, (B): MAL-F1, (C): MAL-F2, (D): MAL-F3, (E): HME-MAL, (F): HME-MAL-F1, (G): HME-MAL-F2, (H): HME-MAL-F3.

lower than when only Probiotics were cultured (Fig. 7A, C). As shown in Fig. 7, the proliferation of probiotics and metabolic activity were increased by HME-MAL-F2 (Fig. 7B, D). The same result of growth of lactic acid bacteria was found when lactic acid bacteria were co-cultured with MAL and HME-MAL-F2.

3.9. Release characteristics of probiotics strains

Rutin and isoquercitrin captured in the HME-MAL-F2 formulation were released into the culture medium in the culture

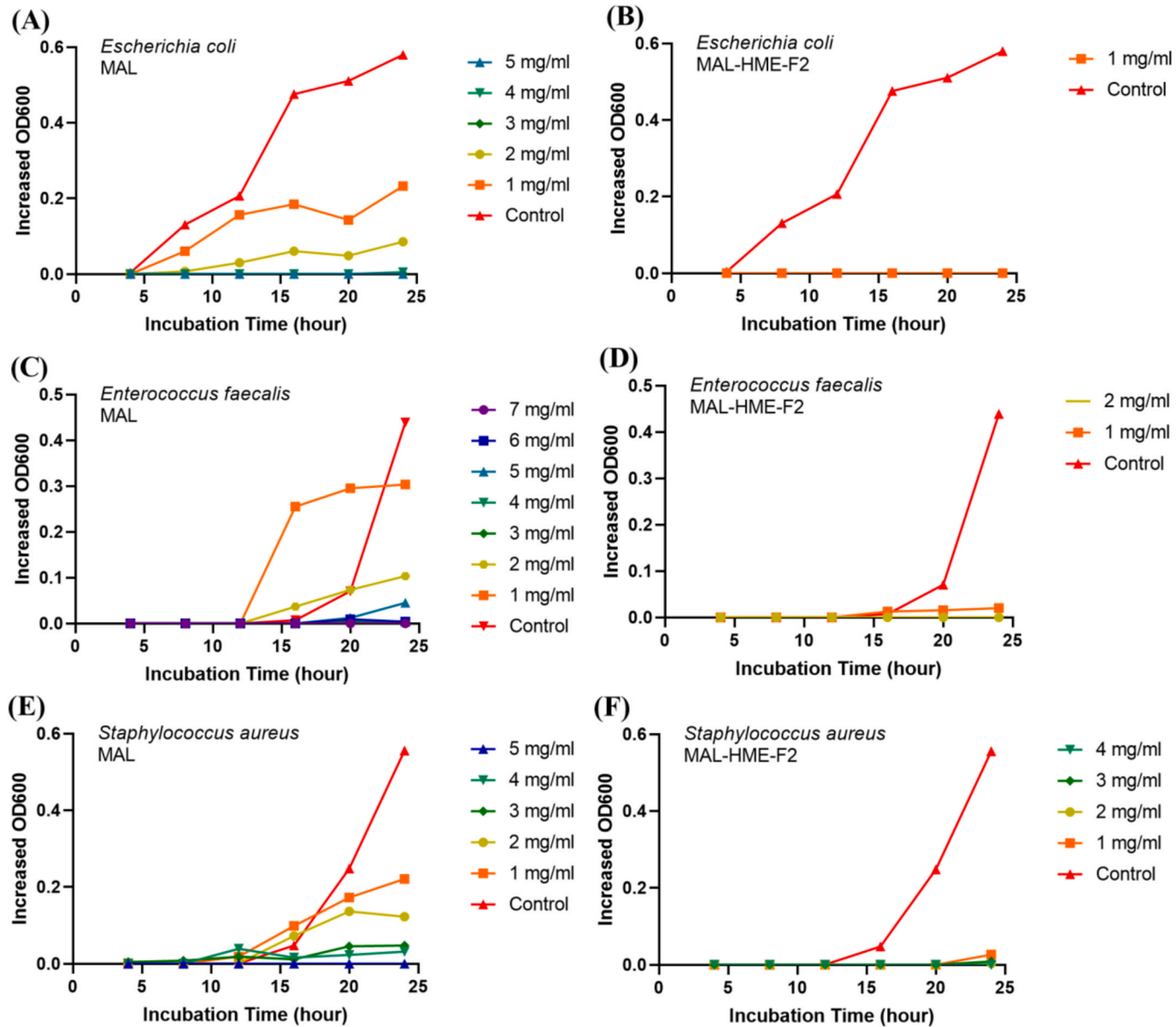


Fig. 5. Growth inhibition effects of *Morus alba* leaf and HME-MAL-F2 on pathogen bacteria. (A, C, E): MAL extract, (B, D, F): HME-MAL-F2 extract, (A, B): treatment of *Escherichia coli*, (C, D): treatment of *Enterococcus faecalis*, (E, F): treatment of *Staphylococcus aureus*.

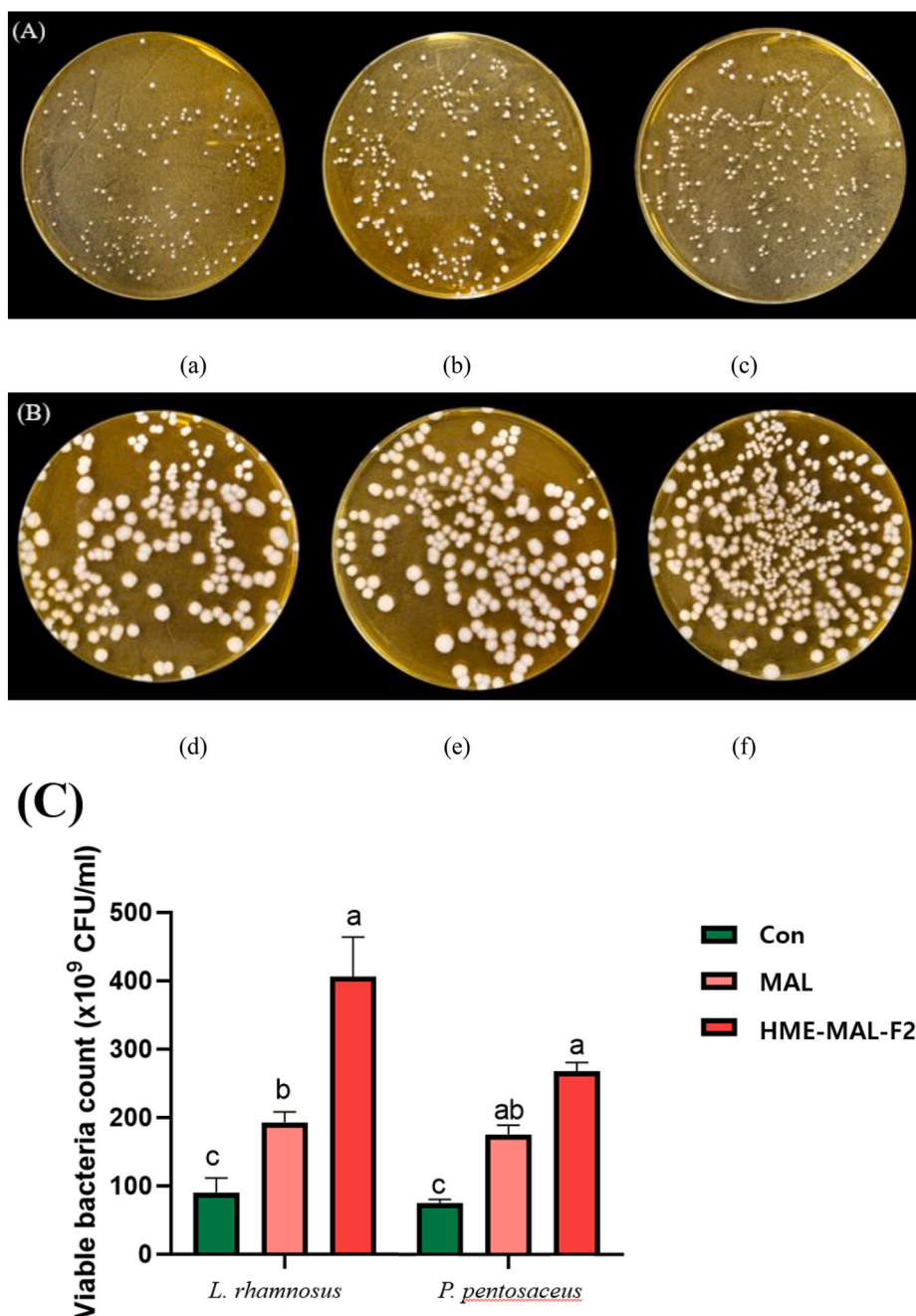


Fig. 6. Photos of probiotics colonies co-cultured with *Morus alba* leaves and HME-MAL-F2. (A) *L. rhamnosus*, (B) *P. pentosaceus*, (C) Number of colonies of probiotics co-cultured with MAL and HME-MAL-F2. (a) *L. rhamnosus*, (b) *L. rhamnosus* + MAL (2 mg/mL), (c) *L. rhamnosus* + HME-MAL-F2 (2 mg/mL), (d) *P. pentosaceus*, (e) *P. pentosaceus* + MAL (2 mg/mL), (f) *P. pentosaceus* + HME-MAL-F2 (2 mg/mL).

environment of *L. rhamnosus* and *P. pentosaceus* and converted into phenolic and organic acids by the metabolism of intestinal microorganisms (Fig. 8A and B). When treating HME-MAL-F2 and MAL, it was confirmed that rutin and isoquercitrin were constantly maintained in the medium over time. It was confirmed that HME-MAL-F2 was maintained at a higher level than MAL. It has also been demonstrated that nanoparticles can be used for antibacterial drug delivery and controlled release [48]. Encapsulation provides a means to control the release of bioactive ingredients with stability, solubility, and bioavailability. It has been demonstrated that different encapsulation techniques of natural bioactive ingredients can enhance their absorption both *in vitro* and *in vivo* [80].

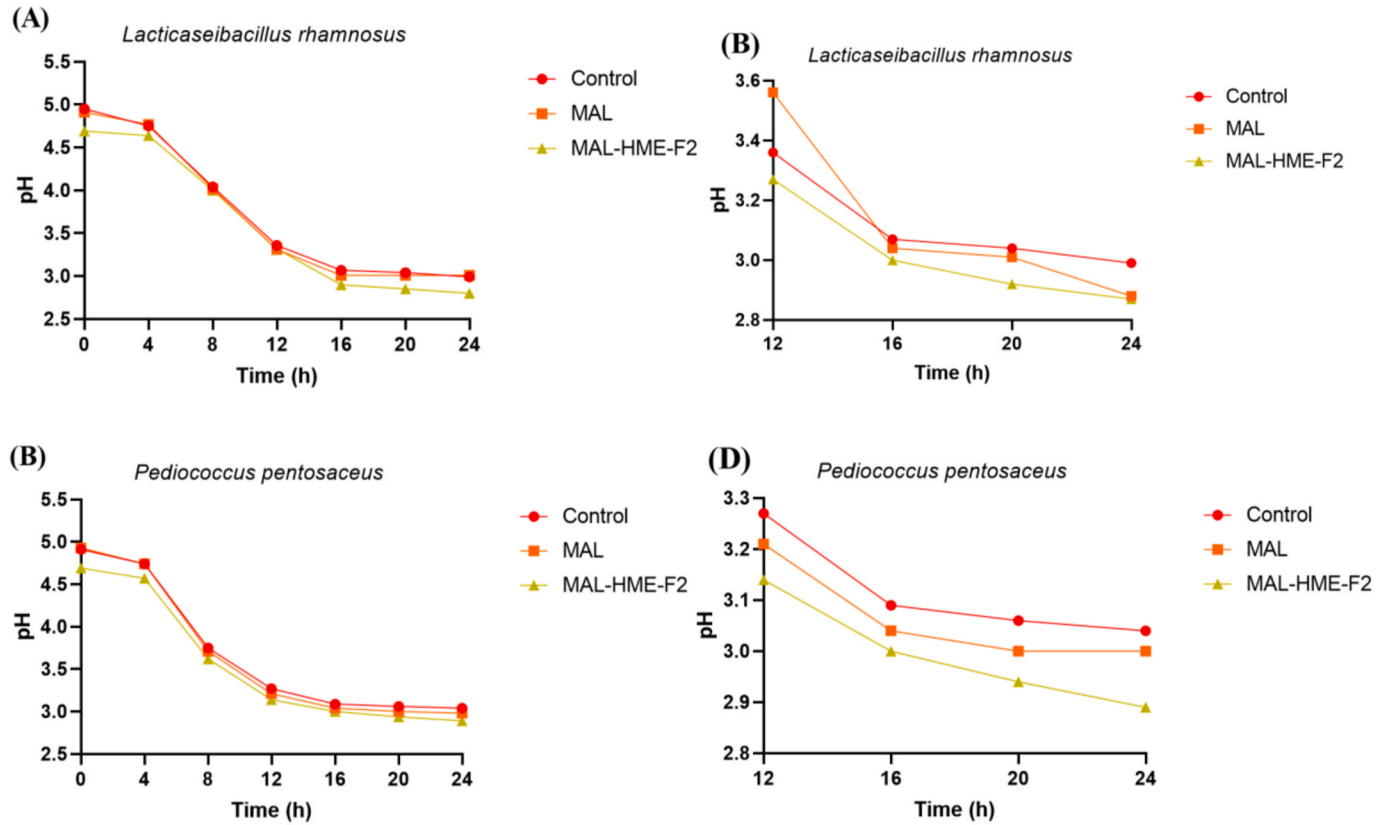


Fig. 7. Changes of pH values of *L. rhamnosus* and *P. pentosaceus* treated with *Morus alba* leaf and HME-MAL-F2. For 24 h, the sample and LAB bacteria were co-cultured in MRS broth. (A, B): *L. rhamnosus* treated with MAL, HME-MAL-F2, (C, D): *P. pentosaceus*. treated with MAL, HME-MAL-F2. (A, C): Treated for 0–24 h, (B, D): Treated for 12–24 h.

3.10. Antibacterial ability of probiotics with HME-MAL-F2

It was confirmed that MAL did not show an antibacterial effect against pathogenic bacteria of *E. coli*, *S. aureus*, or *E. faecalis* (Fig. 9D, E, F, Fig. 10D, E, F). However, it was confirmed that HME-MAL-F2 showed antibacterial activities. Lactic acid bacteria *L. rhamnosus* (Fig. 9) and *P. pentosaceus* (Fig. 10) also showed antibacterial activities. When *L. rhamnosus*, *P. pentosaceus*, and HME-MAL-F2 were simultaneously used for treatment, higher antibacterial activity was found (Fig. 9 A, B, C, Fig. 10A, B, C). These results confirmed that the HME-MAL-F2 formulation with rutin and isoquercitrin as active ingredients exhibited antibacterial effects against pathogenic microorganisms distributed in the intestine and induced proliferation of probiotics. Nanoparticles can affect gut microbiome through interactions with the immune system. These changes in the gut microbiome-immune axis are associated with many chronic diseases, such as inflammatory bowel disease (IBD), diabetes, and even colorectal cancer [81]. It was confirmed that the HME-MAL-F2 formulation can contribute to maintaining the intestinal mucosal barrier because it can maintain the balance of intestinal microflora.

3.11. Toxicities of MAL and HME-mal-f2 to Caco-2 and RAW 264.7 cells

MTT assay was performed to determine toxicities of MAL and HME-MAL-F2 to Caco-2 cells and RAW 264.7 cells. When Caco-2 cells and RAW 264.7 cells reached 80 % confluence, they were treated with MAL and HME-MAL-F2 for 24 h. Next, cytotoxicity was assessed. At doses of 1, 2, and 4 mg/mL, MAL and HME were used. When cells were treated with MAL-F2, cell viability was 100 %. Furthermore, no significant change in cell viability was seen between the untreated and all concentration treatment groups. Experimental results revealed that MAL and HME-MAL-F2 showed low toxicity at 4 mg/mL but no toxicity at 2 mg/mL (Fig. 11A and B). Therefore, they were used in further experiments at a concentration of 2 mg/mL, a concentration that showed an effect in the previous intestinal microbiome improvement experiment.

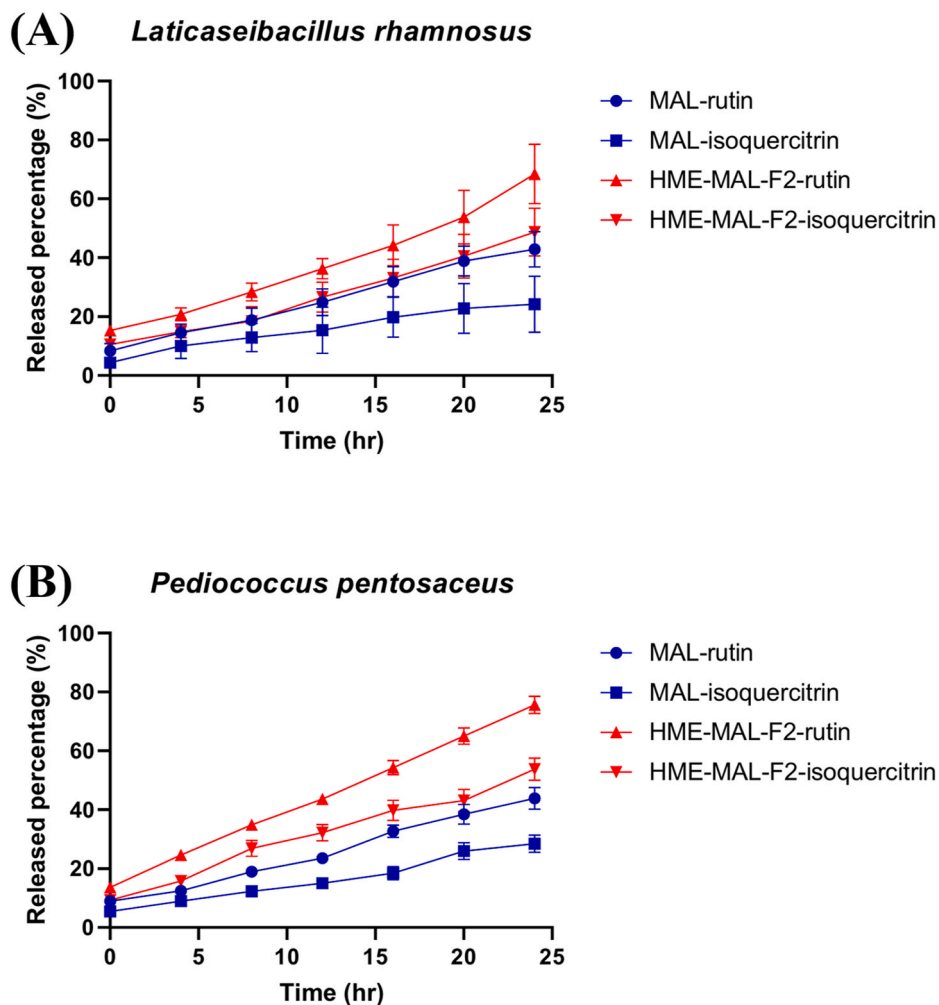


Fig. 8. Released rutin and isoquercitrin contents and release profile of *L. rhamnosus* and *P. pentosaceus* cultured with *Morus alba* leaves and HME-MAL-F2. (A): release profile of *L. rhamnosus*, (B): release profile of *P. pentosaceus*.

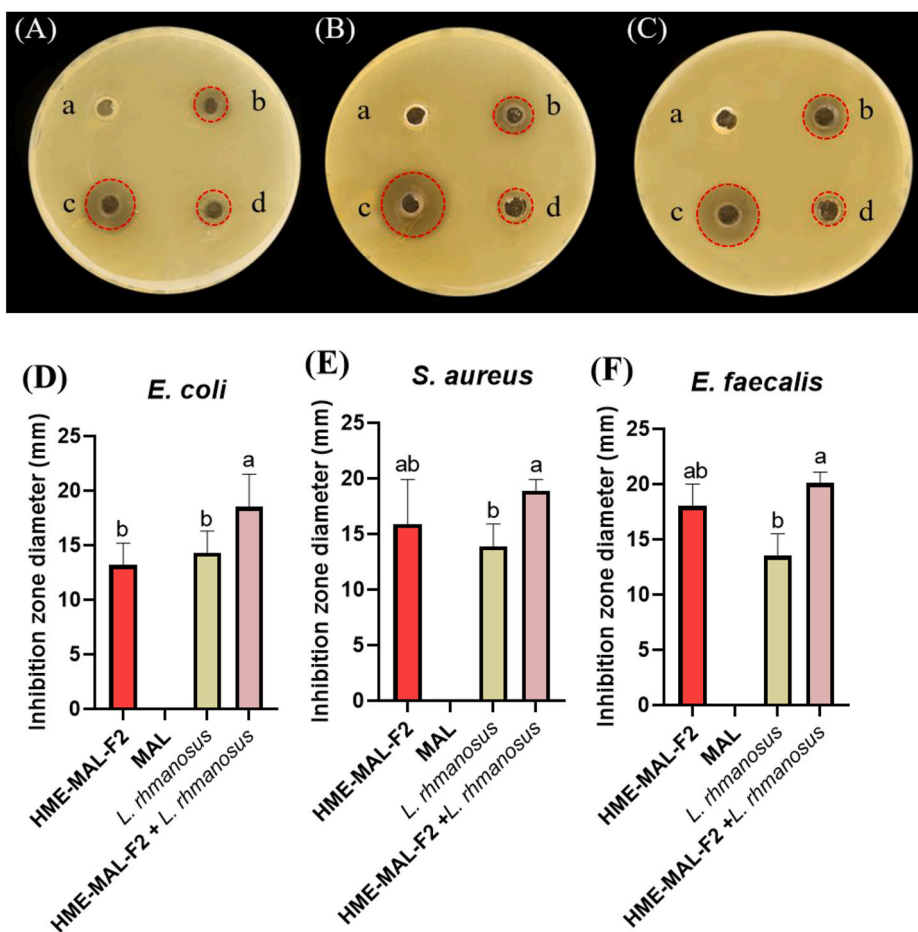


Fig. 9. Inhibition zones when lactic acid bacterium probiotic *L. rhamnosus* is present against test pathogens after treatment with HME-MAL-F2. (A) and (D): Inhibition against *E. coli*; (B) and (E): Inhibition against *S. aureus*; (C) and (F): Inhibition against *E. faecalis*. a: treatment with MAL, b: treatment with HME-MAL-F2, c: treatment with *L. rhamnosus* + HME-MAL-F2, d: treatment with *L. rhamnosus* only. (A)–(C) Photos of clear zones in the presence of probiotics, HME-MAL-F2, and MAL. (D)–(F) Measurement for the width of the inhibition zone under various conditions, including MAL, HME-MAL-F2, probiotics only, and probiotics + HME-MAL-F2.

3.12. Effect of HME-mal-f2 on tight junction integrity of Caco-2 cells

LPS can stimulate the non-specific immune system to cause immune stress, damage tight junctions by expressing intracellular inflammation, and alter the barrier function of the small intestine [82]. It is judged that it can create the same intestinal environment as the small intestine. Under co-culture conditions, when LPS is used to treat the basolateral compartment where RAW 264.7 cells exist, pro-inflammatory cytokines and mediators secreted from RAW 264.7 cells can affect Caco-2 cells, resulting in barrier function impairment through LPS and inflammatory cytokines. An *in vitro* intestinal inflammation model was implemented by treating the basolateral portion with LPS. The degree of damage to tight junction integrity of Caco-2 cells from 0 to 48 h was measured as a transepithelial electrical resistance (TEER) value ($\times \text{cm}^2$). It was confirmed that the integrity of tight junctions was lowered by LPS treatment. To investigate effects of MAL and HME-MAL-F2 on the tight junction integrity of Caco-2 cells, the apical compartment containing Caco-2 cells was pretreated with MAL and HME-MAL-F2 at a concentration of 2 mg/mL, respectively. After treatment with LPS for 48 h, the TEER value was then measured (Fig. 12). When LPS alone was used as treatment without sample pre-treatment, the TEER value was $768 \Omega \times \text{cm}^2$, which was 1.17 times lower than that ($900 \times \text{cm}^2$) of the untreated group (cells only). When LPS was used for treatment, the TEER value of MAL was $842 \Omega \times \text{cm}^2$ and the TEER value of HME-MAL-F2 was $1012 \Omega \times \text{cm}^2$, which were 1.1 and 1.32 times higher than the TEER value of LPS alone, respectively. It was found that the tight junction integrity was decreased by MAL and HME-MAL-F2 as the TEER value over time decreased rapidly immediately after LPS treatment. However, within 2 h, the group treated with MAL returned to a level close to that of the control. In the case of HME-MAL-F2, it was confirmed that the TEER value increased at a statistically significant level compared to MAL. This was because the HME-MAL-F2 formulation showed higher contents of *Morus alba* leaf components due to extrusion and higher penetration into cells [83].

These results were similar to a previous report showing that treatment with *Morus alba* leaves containing flavonoids could reduce the permeability of the TJ induced by LPS [84]. Therefore, *Morus alba* could maintain the membrane permeability of intestinal

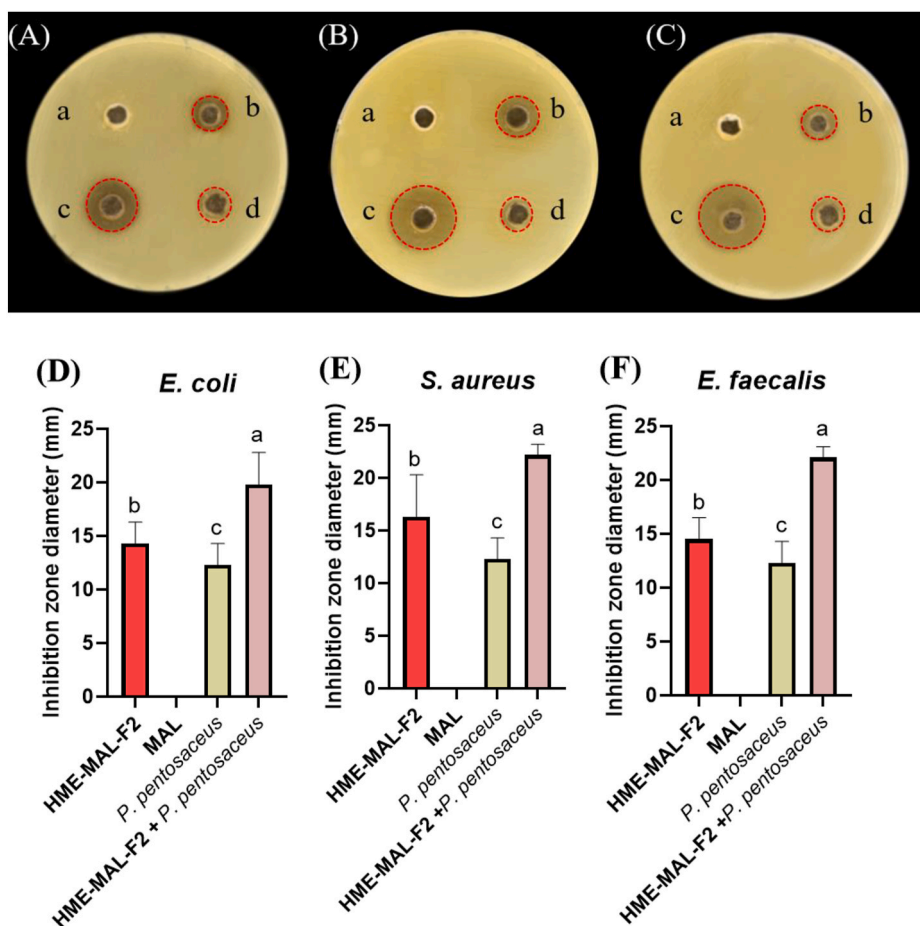


Fig. 10. Following treatment with the HME-DDS formulation (HME-MAL-F2), inhibition zones against test pathogens in the presence of lactic acid bacterial probiotic *P. pentosaceus*. (A) and (D): Inhibition against *E. coli*; (B) and (E): Inhibition against *S. aureus*; (C) and (F): Inhibition against *E. faecalis*. a: treatment with MAL, b: treatment with HME-MAL-F2, c: treatment with *P. pentosaceus* + HME-MAL-F2, d: treatment with *P. pentosaceus* only. (A)–(C) Images of a clean zone in the presence of probiotics, HME-MAL-F2, and MAL. (D)–(F) Quantification of the width of the inhibition zone in the presence of MAL, HME-MAL-F2, probiotics only, and probiotics + HME-MAL-F2, respectively.

epithelial cells. Additionally, we found that the content of iso-quercetin, a component that was difficult to obtain through simple extraction, was increased through HME of *Morus alba* leaves. This component can suppress inflammatory responses in macrophages activated by LPS [85]. Additionally, it is expected that components of *Morus alba* leaves are not damaged or lost despite the heat treatment of HME due to excipient WPI added during formulation [86].

3.13. Effect of HME-mal-f2 on tight junction integrity of Caco-2 cells

In the Caco-2 monolayer in which inflammation was induced by LPS, the decrease in function of tight junctions was confirmed after LPS treatment. However, pretreatment with MAL and HME-MAL-F2 could prevent the loss of integrity of tight junctions caused by LPS. Therefore, when MAL and HME-MAL-F2 were used for treatment, expression levels of inflammatory cytokines in the apical compartment were affected by the mechanism induced by LPS used to treat the basolateral compartment. As a result of measuring the content of cytokine using an ELISA kit, PGE₂ content was 6.14 pg/mL in control cells without any treatment (Fig. 13C). It was 25.09 pg/mL when cells were treated with LPS, showing a 4.1-fold increase in PGE₂ content compared to the untreated group, confirming that the expression of inflammation was induced by LPS. When MAL and LPS were used together to treat the apical compartment, PGE₂ cytokine content was increased again to 19.55 pg/mL, which was reduced by 1.3 times compared to that in the LPS-treated group. When LPS and HME-MAL-F2 were used together to treat cells, PGE₂ content was 8.86 pg/mL, a decrease of 2.83 times. However, it did not recover to the level of the untreated group (Fig. 13). In the case of IL-1 β (Fig. 13B), it was 3.98 pg/mL in the untreated group (cell only). When LPS was used to treat the basolateral compartment, IL-1 β content was 15.83 pg/mL, a 3.98 times increase, indicating that it was secreted from RAW 264.7 cells after LPS treatment. It was confirmed that inflammatory cytokines permeate the membrane, but the level was lowered to 12.42 pg/mL when treated with MAL. It was about 9.18 pg/mL when treated with HME-MAL-F2, which was statistically significant. These results confirmed that anti-inflammatory activities of MAL and HME-MAL-F2 could lower pro-

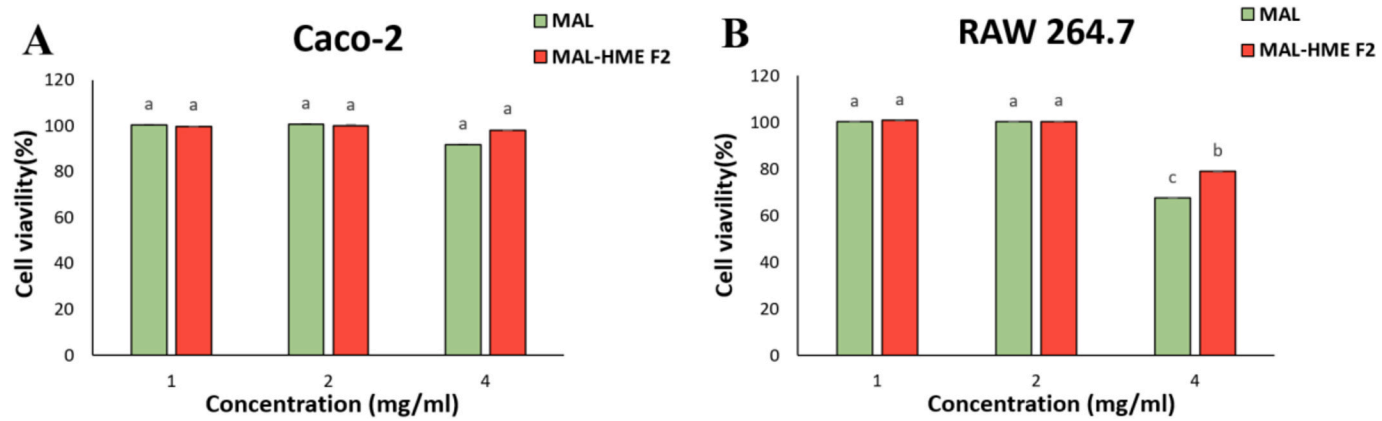


Fig. 11. The effects of HME-MAL-F2 on Caco-2 and RAW 264.7 cell viability. (A): viability of Caco-2 cell, (B): viability of RAW 264.7 cell. Data are presented as means with standard deviations ($n = 3$) compared to 0 mg/mL using a t -test ($p < 0.05$).

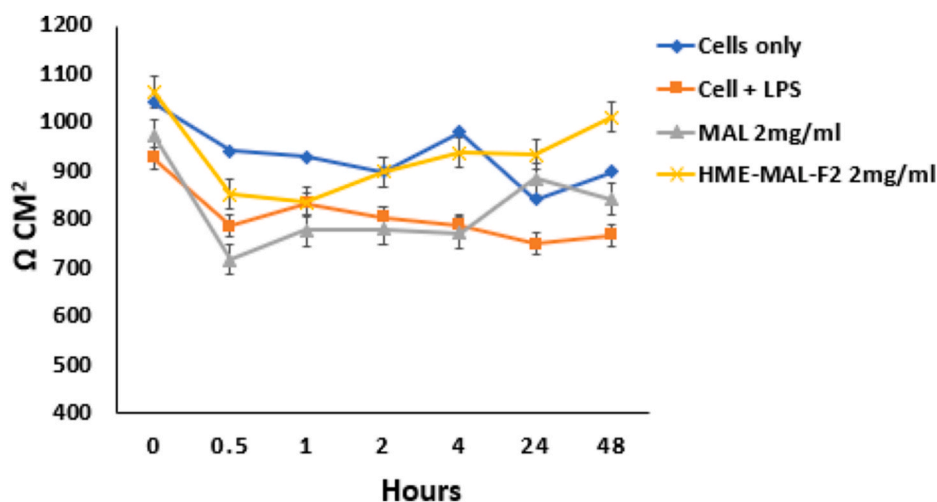


Fig. 12. Preventive effects of HME-MAL-F2 against reduced tight junction integrity induced by treatment with LPS in an *in vitro* gut inflammation model.

inflammatory cytokine levels to levels in the untreated group. HME-DDS formulation showed a higher effect than MAL in maintaining tight junction integrity (Fig. 13). In the case of TNF- α (Fig. 13A), its content was 2.24 pg/mL in the untreated group. It was increased to 11.99 pg/mL after treatment with LPS, 6.45 pg/mL after treatment with MAL, and 4.51 pg/mL after treatment with HME-MAL-F2. Thus, HME-MAL-F2 showed a higher anti-inflammatory effect than MAL at the same concentration (Fig. 13D). It was confirmed that MAL and F2, which inhibit pro-inflammatory cytokines that can induce chronic inflammation, can help improve intestinal mucosal barrier function in LPS-induced inflammation [87]. Since it suppresses the expression of IL-1 β in the LPS-induced inflammation model, we speculate that it will be helpful for the health of the intestinal mucosal barrier. A decrease in pro-inflammatory cytokines was confirmed. Therefore, MAL and HME-MAL-F2 can be used as treatments that can improve intestinal epithelial cells.

It was confirmed that HME-MAL-F2 inhibits the production of pro-inflammatory cytokines at a higher level than MAL. These results indicate that rutin and isoquercitrin have anti-inflammatory effects [88]. It was confirmed that HME-MAL-F2 exhibits a high anti-inflammatory effect, as reported that a solid dispersion using ascorbyl palmitate inhibits TNF- α and exhibits an anti-inflammatory effect. It is judged that the HME-MAL-F2 formulation may be involved in anti-inflammatory activity due to the structural properties of the nanoparticles and the influence of excipients. HME-MAL-F2, which contains alginate and ascorbyl palmitate as excipients, is a controlled release formulation by applying extrusion molding technology. It can improve intestinal barrier function to a higher level than the raw material itself. It can enhance intestinal immune activity to improve intestinal mucosal integrity. And it can be said that it shows potential as a preventive and therapeutic agent for maintaining the health of intestinal immunity from intestinal inflammation.

3.14. Effect of HME-MAL-F2 on expression of genes related to tight junctions

RAW 264.7 cells were administered with LPS in the basolateral compartment to cause an inflammatory response. Expression levels of genes related to tight junctions expressed in Caco-2 cells were determined after pretreatment with MAL and HME-MAL-F2. As a result of checking mRNA levels of TJ-related genes after LPS treatment, compared to the control group (≈ 1), ZO-1 (0.31), Occludin (0.07), JAM-1 (0.31), Claudin-1 (0.16), Claudin-3 (0.05), and Claudin-4 (0.05) mRNA expression levels were reduced. These findings support previous findings that the inflammatory environment induced by LPS treatment, as well as the cytokines produced, can cause the intestinal epithelial barrier to loosen and negatively affect tight junction integrity and morphology by quantitatively suppressing tight junction protein expression and migration [89]. When treated with MAL, ZO-1 increase by 590.0 % (Fig. 14F), Occludin increase by 100 % (Fig. 14B), JAM-1 increase by 66 % (Fig. 14A), Claudin-1 increase by 412.5 % (Fig. 14C), Claudin-3 increase by 580.0 % (Fig. 14D), and Claudin-4 increase by 1500 % compared to those in LPS-treated group were found (Fig. 14E). Expression increase of 10, 040 % for ZO-1, 4242 % increase for Occludin, 490.3 % increase for JAM-1, 238.1 % increase for Claudin-1, 9860 % increase for Claudin-3, and 7420 % increase for Claudin-4 were found after treatment with and HME-MAL-F2. These results indicate that MAL and HME-MAL-F2 can increase the expression levels of tight junction-related genes that were reduced by LPS treatment.

It was confirmed that HME-MAL-F2 could increase the expression of TJ-related genes at a level as high as 2 times. This indicated that the TEER value was higher than that of the raw material when the previously tested HME-DDS formulation was used for treatment. It was confirmed that HME-MAL-F2 can increase the expression of TJ-related genes more than twice. This result supports the previously tested HME-MAL-F2 formulation, in which the TEER value was higher than that of MAL when used for treatment.

TJ, which maintains the intestinal epithelial barrier, is composed of Occludin, ZO-1, Claudin, and JAM proteins that are transmembrane proteins known to interact with the ZO-1 protein to regulate intercellular permeability. It is thought that rutin and isoquercitrin can intervene in the phosphorylation-dephosphorylation process of TJ protein to maintain the intestinal epithelial barrier [90]. In addition, a previous report has shown that flavonoid extracts can upregulate ZO-1, Occludin, claudin-1, -3, and -4 in

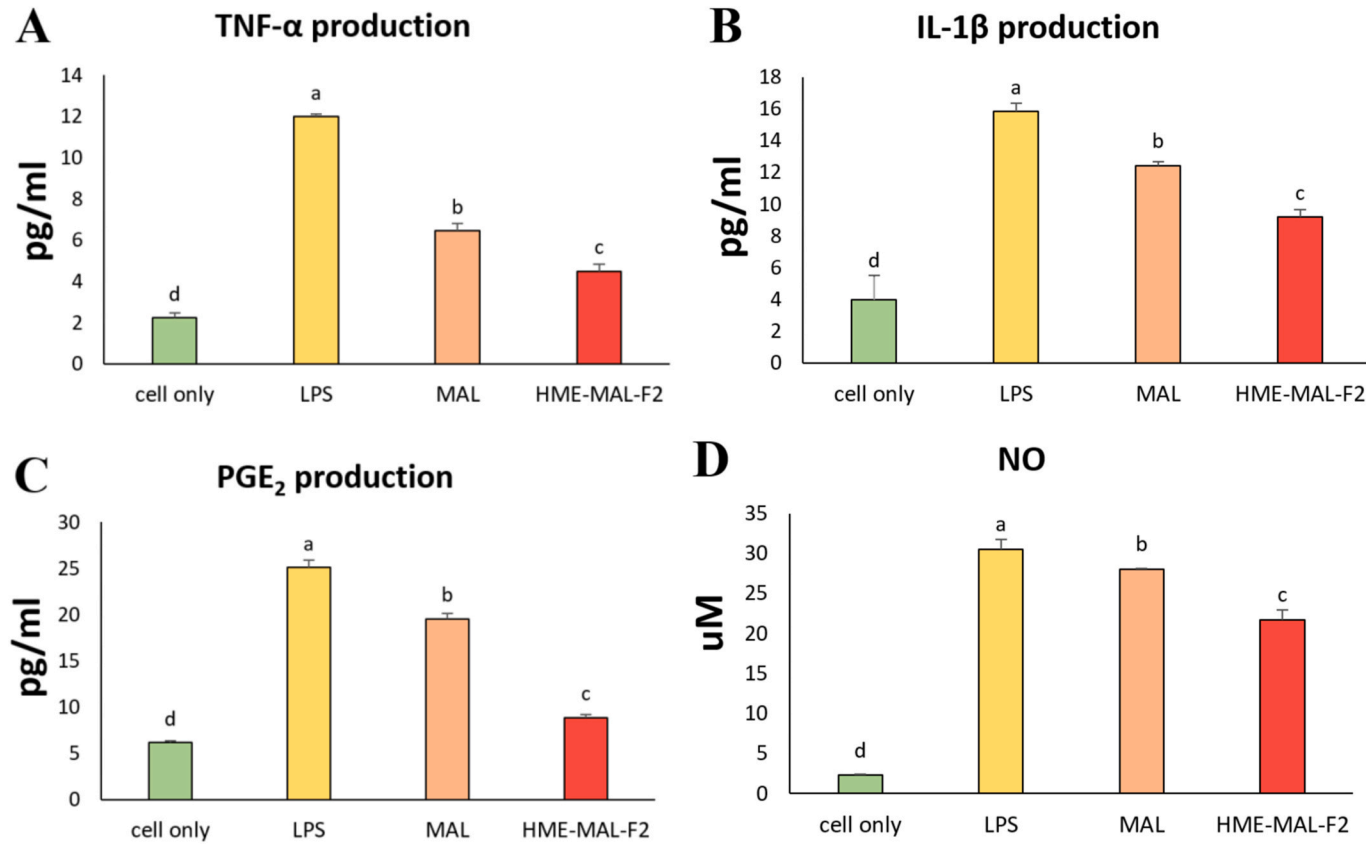


Fig. 13. Effect of HME-MAL-F2 on production of proinflammatory cytokines in Caco-2 cells. ELISA kit analysis results for cytokine production of (A) tumor necrosis factor - α (TNF- α), (B) interleukin1 beta (IL-1 β), (C) prostagrandin E₂ (PGE₂), and (D) NO (nitrite oxide).

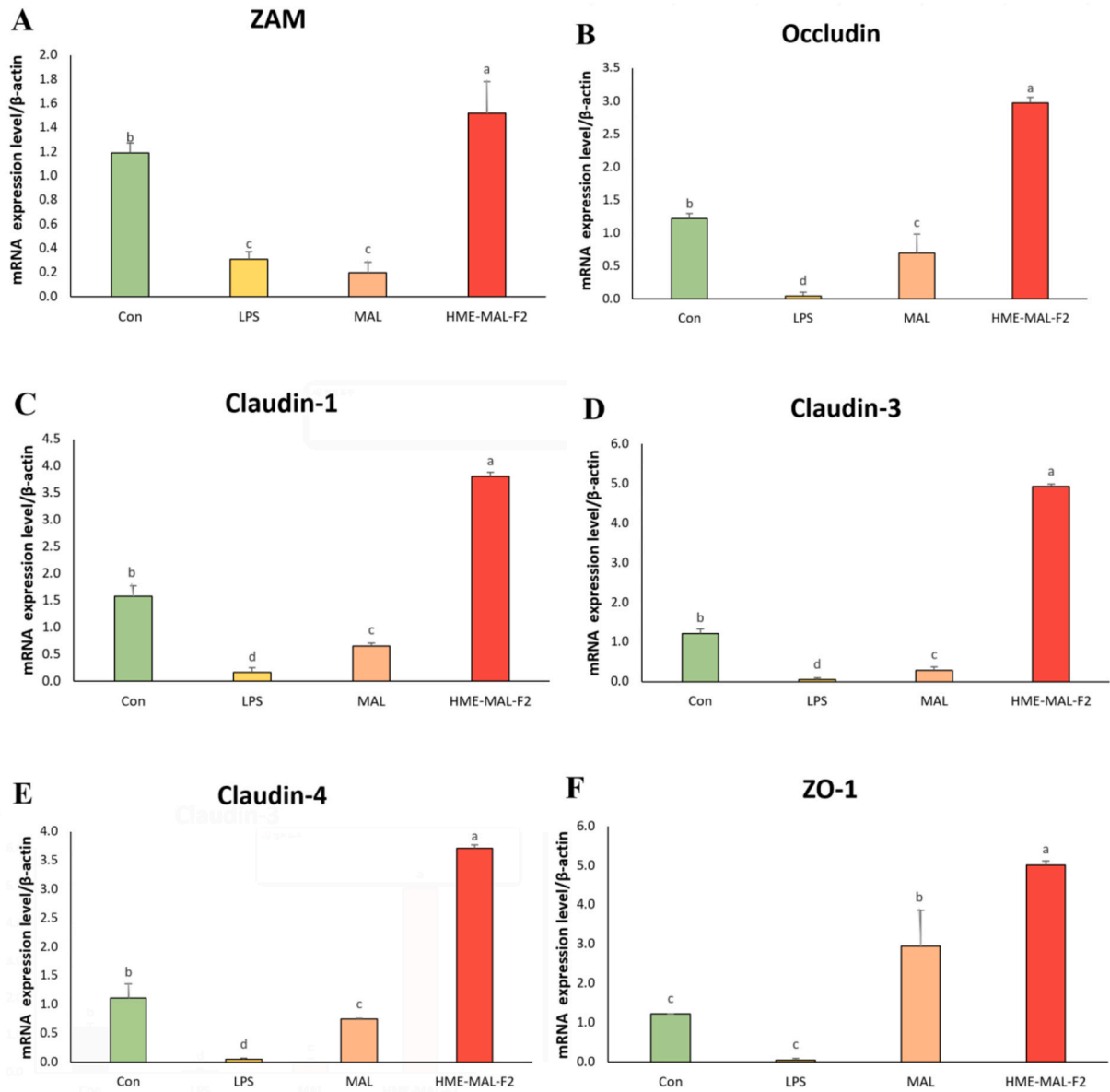


Fig. 14. Comparison of mRNA gene expression of tight junction from HME-MAL-F2 in Caco-2 cells. Using quantitative RT-PCR analysis, transcript levels of tight junction proteins such as (A) ZAM, (B) Occludin, (C) Claudin-1, (D) Claudin-3, (E) Claudin-4, and (F) ZO-1 were examined.

LPS-induced Caco-2 cells [84]. Thus, the increase in mRNA expression in the MAL-treated group might be due to rutin and isoquercetin. The finding that quercetin can improve intestinal TJ barrier integrity and upregulate claudin-4 supports results of MAL [91]. HME-MAL-F2 promoted expression levels of TJ-related genes to higher levels than MAL, which was presumed to be due to the HME technology used for preparing HME-MAL-F2 in addition to flavonoid.

4. Conclusion

In conclusion, it was confirmed that HME-MAL-F2 can increase the content of rutin and isoquercitrin. This high content of bioactive ingredients can affect the proliferation and antibacterial properties of probiotics, resulting in high antibacterial effects. This research demonstrates that the HME-MAL-F2 HME-DDS preparation, which contains active ingredients rutin and isoquercitrin, displays antibacterial effects against harmful bacteria dispersed in the intestine. By preventing the growth of harmful intestinal bacteria and preserving the balance of the complete gut microbiota, it can help keep the mucosal barrier intact. In addition, HME-MAL-F2 is a sustained-release formulation that can increase bioavailability by continuously releasing rutin and isoquercitrin, which have long half-lives, in each part of the gastrointestinal tract. From the above study results, through an *in vitro* gut inflammation model with Caco-2

and RAW 264.7 co-culture, flavonoids contained in *Morus alba* leaves were found to be able to protect and restore the function of tight junctions between damaged intestinal epithelial cells, helping maintain the barrier of the small intestine. HME-DDS formulation (HME-MAL-F2), which contains WPI and ascorbyl palmitate as excipients, is a controlled-release preparation by applying extrusion molding technology. It has a higher level of electrical resistance (transepithelial electrical resistance) of epithelial cells than the raw material itself. It also exhibits anti-inflammatory activity and promotes the expression of genes associated with tight junctions, thereby improving the intestinal barrier function and increasing the activity of intestinal immunity. Thus, it can be used as a preventive and therapeutic agent to maintain and strengthen the integrity of the intestinal mucosa.

5. Data availability

All data generated or analyzed during this study are included in this published article.

CRedit authorship contribution statement

Hyun Bok Kim: Writing - original draft, Project administration, Methodology, Funding acquisition, Formal analysis, Conceptualization. **Eun Ji Go:** Writing - original draft, Methodology, Formal analysis, Conceptualization. **Jong-Suep Baek:** Writing - review & editing, Project administration, Funding acquisition.

Declaration of competing interest

The authors declare that they have no known competing financial interests or personal relationships that could have appeared to influence the work reported in this paper.

Acknowledgment

This research was funded by a grant (PJ015570012023) from the National Institute of Agricultural Sciences, Rural Development Administration, Korea.

References

- [1] S. Nooruddin, S. Kamili, M. Mir, A. Wani, G. Malik, A. Raja, S. Bilal, Seasonal variation in macro nutrient contents of mulberry (*Morus alba*) leaves under temperate climatic conditions of Kashmir, *Int J Agric Innov Res* 4 (2015) 147–152.
- [2] Y. Lin, C. Wu, P. Kuo, W. Chen, J.T.C. Tzen, Quercetin 3-O-malonylglucoside in the leaves of mulberry (*Morus alba*) is a functional analog of ghrelin, *J. Food Biochem.* 44 (2020), e13379.
- [3] E.W.-C. Chan, L.Y.E. Phui-Yan, W. Siu-Kuin, Phytochemistry, pharmacology, and clinical trials of *Morus alba*, *Chin. J. Nat. Med.* 14 (2016) 17–30.
- [4] A.G. Junior, T.B.L. Prando, T. dos, S.V. Leme, F.M. Gasparotto, E.L.B. Lourenço, Y.D. Rattmann, J.E. Da Silva-Santos, C.A.L. Kassuya, M.C.A. Marques, Mechanisms underlying the diuretic effects of *Tropaeolum majus* L. extracts and its main component isoquercitrin, *J. Ethnopharmacol.* 141 (2012) 501–509.
- [5] L. Weignerová, P. Marhol, D. Gerstorferová, V. Křen, Preparatory production of quercetin-3- β -D-glucopyranoside using alkali-tolerant thermostable α -L-rhamnosidase from *Aspergillus terreus*, *Bioresour. Technol.* 115 (2012) 222–227.
- [6] A. Mukherji, A. Kobiita, T. Ye, P. Chambon, Homeostasis in intestinal epithelium is orchestrated by the circadian clock and microbiota cues transduced by TLRs, *Cell* 153 (2013) 812–827.
- [7] R. Sender, S. Fuchs, R. Milo, Revised estimates for the number of human and bacteria cells in the body, *PLoS Biol.* 14 (2016), e1002533.
- [8] A.T. Soderholm, V.A. Pedicord, Intestinal epithelial cells: at the interface of the microbiota and mucosal immunity, *Immunology* 158 (2019) 267–280.
- [9] S. V Lynch, O. Pedersen, The human intestinal microbiome in health and disease, *N. Engl. J. Med.* 375 (2016) 2369–2379.
- [10] D. Berg, J.C. Clemente, J.-F. Colombel, Can inflammatory bowel disease be permanently treated with short-term interventions on the microbiome? *Expert Rev Gastroenterol Hepatol* 9 (2015) 781–795.
- [11] B. Allam-Ndoul, S. Castonguay-Paradis, A. Veilleux, Gut microbiota and intestinal trans-epithelial permeability, *Int. J. Mol. Sci.* 21 (2020) 6402.
- [12] E.E. Blaak, E.E. Canfora, S. Theis, G. Frost, A.K. Groen, G. Mithieux, A. Nauta, K. Scott, B. Stahl, J. Van Harsselaar, Short chain fatty acids in human gut and metabolic health, *Benef. Microbes* 11 (2020) 411–455.
- [13] C. Martin-Gallausiaux, L. Marinelli, H.M. Blottière, P. Larrauffe, N. Lapaque, SCFA: mechanisms and functional importance in the gut, *Proc. Nutr. Soc.* 80 (2021) 37–49.
- [14] J. Von Moltke, M. Ji, H.-E. Liang, R.M. Locksley, Tuft-cell-derived IL-25 regulates an intestinal ILC2–epithelial response circuit, *Nature* 529 (2016) 221–225.
- [15] H. Gehart, H. Clevers, Tales from the crypt: new insights into intestinal stem cells, *Nat. Rev. Gastroenterol. Hepatol.* 16 (2019) 19–34.
- [16] S.D. Viana, S. Nunes, F. Reis, ACE2 imbalance as a key player for the poor outcomes in COVID-19 patients with age-related comorbidities—role of gut microbiota dysbiosis, *Ageing Res. Rev.* 62 (2020), 101123.
- [17] Y.H. Kwon, H. Wang, E. Denou, J.-E. Ghia, L. Rossi, M.E. Fontes, S.P. Bernier, M.S. Shajib, S. Banskota, S.M. Collins, Modulation of gut microbiota composition by serotonin signaling influences intestinal immune response and susceptibility to colitis, *Cell Mol Gastroenterol Hepatol* 7 (2019) 709–728.
- [18] D.M. Alvarado, B. Chen, M. Iticovici, A.I. Thaker, N. Dai, K.L. VanDussen, N. Shaikh, C.K. Lim, G.J. Guillemin, P.I. Tarr, Epithelial indoleamine 2, 3-dioxygenase 1 modulates aryl hydrocarbon receptor and notch signaling to increase differentiation of secretory cells and alter mucus-associated microbiota, *Gastroenterology* 157 (2019) 1093–1108.
- [19] W.A. Petri, M. Miller, H.J. Binder, M.M. Levine, R. Dillingham, R.L. Guerrant, Enteric infections, diarrhea, and their impact on function and development, *J. Clin. Invest.* 118 (2008) 1277–1290.
- [20] C. Wang, Q. Li, J. Ren, Microbiota-immune interaction in the pathogenesis of gut-derived infection, *Front. Immunol.* 10 (2019) 1873.
- [21] Q.R. Ducarmon, R.D. Zwitterink, B.V.H. Hornung, W. Van Schaik, V.B. Young, E.J. Kuijper, Gut microbiota and colonization resistance against bacterial enteric infection, *Microbiol. Mol. Biol. Rev.* 83 (2019), e00007-19.
- [22] Y. Goto, I.I. Ivanov, Intestinal epithelial cells as mediators of the commensal–host immune crosstalk, *Immunol. Cell Biol.* 91 (2013) 204–214.
- [23] S.M. Nabavi, A.S. Silva, Nonvitamin and Nonmineral Nutritional Supplements, Academic Press, 2018.
- [24] Y. Huang, W.-G. Dai, Fundamental aspects of solid dispersion technology for poorly soluble drugs, *Acta Pharm. Sin. B* 4 (2014) 18–25.
- [25] Y. Mori, K. Motoyama, M. Ishida, R. Onodera, T. Higashi, H. Arima, Theoretical and practical evaluation of lowly hydrolyzed polyvinyl alcohol as a potential carrier for hot-melt extrusion, *Int J Pharm* 555 (2019) 124–134.

- [26] N. Chowdhury, I. Vhora, K. Patel, A. Bagde, S. Kotlehria, M. Singh, Development of hot melt extruded solid dispersion of tamoxifen citrate and resveratrol for synergistic effects on breast cancer cells, *AAPS PharmSciTech* 19 (2018) 3287–3297.
- [27] K. Ishimoto, S. Miki, A. Ohno, Y. Nakamura, S. Otani, M. Nakamura, S. Nakagawa, β -Carotene solid dispersion prepared by hot-melt technology improves its solubility in water, *J. Food Sci. Technol.* 56 (2019) 3540–3546.
- [28] M.A. Repka, S. Bandari, V.R. Kallakunta, A.Q. Vo, H. McFall, M.B. Pimparade, A.M. Bhagurkar, Melt extrusion with poorly soluble drugs—An integrated review, *Int J Pharm* 535 (2018) 68–85.
- [29] B. Bin Huang, D.X. Liu, D.K. Liu, G. Wu, Application of solid dispersion technique to improve solubility and sustain release of emamectin benzoate, *Molecules* 24 (2019) 4315.
- [30] Y.-S. Lee, J.G. Song, S.H. Lee, H.-K. Han, Sustained-release solid dispersion of pelubiprofen using the blended mixture of aminoclay and pH independent polymers: preparation and in vitro/in vivo characterization, *Drug Deliv.* 24 (2017) 1731–1739.
- [31] D. V. Zelikina, M.D. Gureeva, S.A. Chebotarev, Y. V Samuseva, A.S. Antipova, E.I. Martirosova, M.G. Semenova, Functional food compositions based on whey protein isolate, fish oil and soy phospholipids, *Food Systems* 3 (2020) 16–20.
- [32] F. Wu, F. Chen, Y. Pu, F. Qian, Y. Leng, G. Mu, X. Zhu, Effects of soy lecithin concentration on the physicochemical properties of whey protein isolate, casein-stabilised simulated infant formula emulsion and their corresponding microcapsules, *Int. J. Dairy Technol.* 75 (2022) 513–526.
- [33] A.M. Chuah, B. Jacob, Z. Jie, S. Ramesh, S. Mandal, J.K. Puthan, P. Deshpande, V. V Vaidyanathan, R.W. Gelling, G. Patel, Enhanced bioavailability and bioefficacy of an amorphous solid dispersion of curcumin, *Food Chem.* 156 (2014) 227–233.
- [34] Q.D. Do, A.E. Angkawijaya, P.L. Tran-Nguyen, L.H. Huynh, F.E. Soetaredjo, S. Ismadji, Y.-H. Ju, Effect of extraction solvent on total phenol content, total flavonoid content, and antioxidant activity of *Limnophila aromatica*, *J. Food Drug Anal.* 22 (2014) 296–302.
- [35] J.-D. Lim, C.-Y. Yu, M.-J. Kim, S.-J. Yun, S.-J. Lee, N.-Y. Kim, I.-M. Chung, Comparison of SOD activity and phenolic compound contents in various Korean medicinal plants, *Korean Journal of Medicinal Crop Science* 12 (2004) 191–202.
- [36] A.J. Vlietinck, Screening methods for antibacterial and antiviral agents from higher plants, in: *Methods in Plant Biochemistry/Hostettmann, K.[Edit.]*, 1991, pp. 47–69.
- [37] K. Ishii, S. Nakamura, Y. Sato, Measurement of dispersion of nanoparticles in a dense suspension by high-sensitivity low-coherence dynamic light scattering, in: *International Conference on Optical Particle Characterization (OPC 2014)*, SPIE, 2014, pp. 94–99.
- [38] K. Chaitanya, Molecular structure, vibrational spectroscopic (FT-IR, FT-Raman), UV–vis spectra, first order hyperpolarizability, NBO analysis, HOMO and LUMO analysis, thermodynamic properties of benzophenone 2, 4-dicarboxylic acid by ab initio HF and density functional method, *Spectrochim. Acta Mol. Biomol. Spectrosc.* 86 (2012) 159–173.
- [39] M. Jin, W.-J. Jeon, H. Lee, M. Jung, H.-E. Kim, H. Yoo, J.-H. Won, J.C. Kim, J.-H. Park, M.-J. Yang, Preparation and evaluation of rapid disintegrating formulation from coated microneedle, *Drug Deliv Transl Res* (2021) 1–11.
- [40] A. Olejnik, K. Kowalska, M. Olkiewicz, J. Rychlik, W. Juzwa, K. Myszka, R. Dembczyński, W. Białas, Anti-inflammatory effects of gastrointestinal digested *Sambucus nigra* L. fruit extract analysed in co-cultured intestinal epithelial cells and lipopolysaccharide-stimulated macrophages, *J. Funct.Foods* 19 (2015) 649–660.
- [41] J.A. Baird, L.S. Taylor, Evaluation of amorphous solid dispersion properties using thermal analysis techniques, *Adv. Drug Deliv. Rev.* 64 (2012) 396–421.
- [42] A.K. Nayak, M.S. Hasnain, *Alginates in Drug Delivery*, Academic Press, 2020.
- [43] W. Liu, X.D. Chen, Z. Cheng, C. Selomulya, On enhancing the solubility of curcumin by microencapsulation in whey protein isolate via spray drying, *J. Food Eng.* 169 (2016) 189–195.
- [44] C. Tang, Assembled milk protein nano-architectures as potential nanovehicles for nutraceuticals, *Adv. Colloid Interface Sci.* 292 (2021), 102432.
- [45] K.N.P. Humblet-Hua, G. Schellens, E. Van Der Linden, L.M.C. Sagis, Encapsulation systems based on ovalbumin fibrils and high methoxyl pectin, *Food Hydrocoll* 25 (2011) 569–576.
- [46] M. Subirade, L. Chen, Food-protein-derived materials and their use as carriers and delivery systems for active food components. *Delivery and Controlled Release of Bioactives in Foods and Nutraceuticals*, 2008, pp. 251–278.
- [47] E.-J. Go, B.-R. Ryu, S.-J. Ryu, H.-B. Kim, H.-T. Lee, J.-W. Kwon, J.-S. Baek, J.-D. Lim, An enhanced water solubility and stability of anthocyanins in mulberry processed with hot melt extrusion, *Int. J. Mol. Sci.* 22 (2021), 12377.
- [48] M.U. Amin, M. Khurram, B. Khattak, J. Khan, Antibiotic additive and synergistic action of rutin, morin and quercetin against methicillin resistant *Staphylococcus aureus*, *BMC Compl. Alternative Med.* 15 (2015) 1–12.
- [49] G. Verreck, The Influence of Plasticizers in Hot-Melt Extrusion, *Hot-Melt Extrusion, Pharmaceutical Applications*, 2012, pp. 93–112.
- [50] K. Adavallan, N. Krishnakumar, Mulberry leaf extract mediated synthesis of gold nanoparticles and its anti-bacterial activity against human pathogens, *Adv. Nat. Sci. Nanosci. Nanotechnol.* 5 (2014), 025018.
- [51] H. Yong, X. Wang, R. Bai, Z. Miao, X. Zhang, J. Liu, Development of antioxidant and intelligent pH-sensing packaging films by incorporating purple-fleshed sweet potato extract into chitosan matrix, *Food Hydrocoll* 90 (2019) 216–224.
- [52] G. Rajakumar, A.A. Rahuman, Larvicidal activity of synthesized silver nanoparticles using *Eclipta prostrata* leaf extract against filariasis and malaria vectors, *Acta Trop.* 118 (2011) 196–203.
- [53] J. Chen, L. Li, X. Zhou, B. Li, X. Zhang, R. Hui, Structural characterization and α -glucosidase inhibitory activity of polysaccharides extracted from Chinese traditional medicine *Huidouba*, *Int. J. Biol. Macromol.* 117 (2018) 815–819.
- [54] M.K. Murali, V. Balachandran, FT-IR, FT-Raman, DFT Structure, Vibrational Frequency Analysis and Mulliken Charges of 2-chlorophenylisothiocyanate, 2012.
- [55] M. Sirajuddin, S. Ali, A. Shah Nawaz, F. Perveen, S. Andleeb, S. Ali, Exploration of biological potency of carboxylic acid derivatives: designing, synthesis, characterizations and molecular docking study, *J. Mol. Struct.* 1207 (2020), 127809.
- [56] L. Netchacovitch, E. Dumont, J. Caillaud, J. Thiry, C. De Bleye, P.-Y. Sacré, M. Boiret, B. Evrard, P.H. Hubert, E. Ziemons, Development of an analytical method for crystalline content determination in amorphous solid dispersions produced by hot-melt extrusion using transmission Raman spectroscopy: a feasibility study, *Int J Pharm* 530 (2017) 249–255.
- [57] Y. Liu, Y. Qin, R. Bai, X. Zhang, L. Yuan, J. Liu, Preparation of pH-sensitive and antioxidant packaging films based on κ -carrageenan and mulberry polyphenolic extract, *Int. J. Biol. Macromol.* 134 (2019) 993–1001.
- [58] T. Lei, J. Shin, D.S. Gianola, T.J. Rupert, Bulk nanocrystalline Al alloys with hierarchical reinforcement structures via grain boundary segregation and complex formation, *Acta Mater.* 221 (2021), 117394.
- [59] Y. Zhang, M. Yang, N.G. Portney, D. Cui, G. Budak, E. Ozbay, M. Ozkan, C.S. Ozkan, Zeta potential: a surface electrical characteristic to probe the interaction of nanoparticles with normal and cancer human breast epithelial cells, *Biomed. Microdevices* 10 (2008) 321–328.
- [60] J. Breitenbach, Melt extrusion: from process to drug delivery technology, *Eur. J. Pharm. Biopharm.* 54 (2002) 107–117.
- [61] N. Li, C.J. Gilpin, L.S. Taylor, Understanding the impact of water on the miscibility and microstructure of amorphous solid dispersions: an AFM–LCR and TEM–EDX study, *Mol. Pharm.* 14 (2017) 1691–1705.
- [62] S.A. Khan, X. Ma, S. V Jermain, H. Ali, I.A. Khalil, M. El Fouly, A.H. Osman, R.O. Williams III, Sustained release biocompatible ocular insert using hot melt extrusion technology: fabrication and in-vivo evaluation, *J. Drug Deliv. Sci. Technol.* 71 (2022), 103333.
- [63] M. Mehta, S.P. Bhardwaj, R. Suryanarayanan, Controlling the physical form of mannitol in freeze-dried systems, *Eur. J. Pharm. Biopharm.* 85 (2013) 207–213.
- [64] A.A. Mostafa, A.A. Al-Askar, K.S. Almaary, T.M. Dawoud, E.N. Sholkamy, M.M. Bakri, Antimicrobial activity of some plant extracts against bacterial strains causing food poisoning diseases, *Saudi J. Biol. Sci.* 25 (2018) 361–366.
- [65] A. Gryn-Rynko, I. Holyńska-Iwan, M.A. Janiak, D. Olszewska-Stonina, R. Amarowicz, R. Graczyk, The impact of *Morus alba* L. leaf extract on intestinal ion transport. An in vitro study, *Biomed. Pharmacother.* 150 (2022), 112939.
- [66] S. Cai, W. Sun, Y. Fan, X. Guo, G. Xu, T. Xu, Y. Hou, B. Zhao, X. Feng, T. Liu, Effect of mulberry leaf (*Folium Mori*) on insulin resistance via IRS-1/PI3K/Glut-4 signalling pathway in type 2 diabetes mellitus rats, *Pharm. Biol.* 54 (2016) 2685–2691.

- [67] A.M. de Oliveira, M. da Silva Mesquita, G.C. da Silva, E. de Oliveira Lima, P.L. de Medeiros, P.M.G. Paiva, I.A. de Souza, T.H. Napoleao, Evaluation of Toxicity and Antimicrobial Activity of an Ethanolic Extract from Leaves of *Morus Alba* L, Evidence-Based Complementary and Alternative Medicine, 2015, p. 2015.
- [68] X. Zhang, Y. Yang, Z. Wu, P. Weng, The modulatory effect of anthocyanins from purple sweet potato on human intestinal microbiota in vitro, *J. Agric. Food Chem.* 64 (2016) 2582–2590.
- [69] J.C. Clemente, J. Manasson, J.U. Scher, The role of the gut microbiome in systemic inflammatory disease, *Bmj* 360 (2018).
- [70] J.A. Vanderhoof, R. Young, Probiotics in the United States, *Clin. Infect. Dis.* 46 (2008) S67–S72.
- [71] S.-I. Ahn, S. Cho, N.-J. Choi, Effect of dietary probiotics on colon length in an inflammatory bowel disease–induced murine model: a meta-analysis, *J. Dairy Sci.* 103 (2020) 1807–1819.
- [72] S. Jiang, L. Cai, L. Lv, L. Li, *Pediococcus pentosaceus*, a future additive or probiotic candidate, *Microb Cell Fact* 20 (2021) 1–14.
- [73] J.H. Saadoun, L. Calani, M. Cirlini, V. Bernini, E. Neviani, D. Del Rio, G. Galaverna, C. Lazzi, Effect of fermentation with single and co-culture of lactic acid bacteria on okara: evaluation of bioactive compounds and volatile profiles, *Food Funct.* 12 (2021) 3033–3043.
- [74] L. Chebil, M. Bouroukba, C. Gaiani, C. Charbonel, M. Khaldi, J.-M. Engasser, M. Ghoul, Elucidation of the kinetic behavior of quercetin, isoquercitrin, and rutin solubility by physicochemical and thermodynamic investigations, *Ind. Eng. Chem. Res.* 52 (2013) 1464–1470.
- [75] E.J. Go, B.R. Ryu, G.J. Gim, H.Y. Lee, H.S. You, H.B. Kim, H.T. Lee, J.Y. Lee, M.S. Shim, J.-S. Baek, Hot-melt extrusion enhances antioxidant effects of mulberry on probiotics and pathogenic microorganisms, *Antioxidants* 11 (2022) 2301.
- [76] E. Chenoll, I. Moreno, M. Sánchez, I. Garcia-Grau, A. Silva, M. González-Monfort, S. Genovés, F. Vilella, C. Seco-Durban, C. Simón, Selection of new probiotics for endometrial health, *Front. Cell. Infect. Microbiol.* 9 (2019) 114.
- [77] J. van Duynhoven, E.E. Vaughan, D.M. Jacobs, R.A. Kemperman, E.J.J. van Velzen, G. Gross, L.C. Roger, S. Possemiers, A.K. Smilde, J. Doré, Metabolic fate of polyphenols in the human superorganism, *Proc. Natl. Acad. Sci. USA* 108 (2011) 4531–4538.
- [78] F.A. Tomás-Barberán, J.C. Espín, Effect of food structure and processing on (Poly) phenol–gut microbiota interactions and the effects on human health, *Annu. Rev. Food Sci. Technol.* 10 (2019) 221–238.
- [79] Y. Liu, H. Cheng, H. Liu, R. Ma, J. Ma, H. Fang, Fermentation by multiple bacterial strains improves the production of bioactive compounds and antioxidant activity of goji juice, *Molecules* 24 (2019) 3519.
- [80] P. Basnet, N. Skalko-Basnet, Nanodelivery systems for improved topical antimicrobial therapy, *Curr Pharm Des* 19 (2013) 7237–7243.
- [81] M.L. Richard, G. Liguori, B. Lamas, G. Brandi, G. Da Costa, T.W. Hoffmann, M. Pierluigi Di Simone, C. Calabrese, G. Poggioli, P. Langella, Mucosa-associated microbiota dysbiosis in colitis associated cancer, *Gut Microb.* 9 (2018) 131–142.
- [82] R. Nallathambi, A. Poulev, J.B. Zuk, I. Raskin, Proanthocyanidin-rich grape seed extract reduces inflammation and oxidative stress and restores tight junction barrier function in Caco-2 colon cells, *Nutrients* 12 (2020) 1623.
- [83] H.-B. Kim, S. Ryu, J.-S. Baek, The effect of hot-melt extrusion of mulberry leaf on the number of active compounds and antioxidant activity, *Plants* 11 (2022) 3019.
- [84] S. Gong, J. Zheng, J. Zhang, Y. Wang, Z. Xie, Y. Wang, J. Han, Taxifolin ameliorates lipopolysaccharide-induced intestinal epithelial barrier dysfunction via attenuating NF-kappa B/MLCK pathway in a Caco-2 cell monolayer model, *Food Res. Int.* 158 (2022), 111502.
- [85] S.-J. Choi, B.H. Tai, N.M. Cuong, Y.-H. Kim, H.-D. Jang, Antioxidative and anti-inflammatory effect of quercetin and its glycosides isolated from *mampat* (*Cratogeomys formosum*), *Food Sci. Biotechnol.* 21 (2012) 587–595.
- [86] X. Chen, Y. Guan, M. Zeng, Z. Wang, F. Qin, J. Chen, Z. He, Effect of whey protein isolate and phenolic copigments in the thermal stability of mulberry anthocyanin extract at an acidic pH, *Food Chem.* 377 (2022), 132005.
- [87] V. Umare, V. Pradhan, M. Nadkar, A. Rajadhyaksha, M. Patwardhan, K.K. Ghosh, A.H. Nadkarni, Effect of proinflammatory cytokines (IL-6, TNF- α , and IL-1 β) on clinical manifestations in Indian SLE patients, *Mediators Inflamm* 2014 (2014).
- [88] S.-S. Choi, H.-R. Park, K. Lee, A comparative study of rutin and rutin glycoside: antioxidant activity, anti-inflammatory effect, effect on platelet aggregation and blood coagulation, *Antioxidants* 10 (2021) 1696.
- [89] A. Watari, Y. Sakamoto, K. Hisaie, K. Iwamoto, M. Fueta, K. Yagi, M. Kondoh, Rebecamycin attenuates TNF- α -induced intestinal epithelial barrier dysfunction by inhibiting myosin light chain kinase production, *Cell. Physiol. Biochem.* 41 (2017) 1924–1934.
- [90] T. Suzuki, Regulation of the intestinal barrier by nutrients: the role of tight junctions, *Anim. Sci. J.* 91 (2020), e13357.
- [91] T. Suzuki, Regulation of intestinal epithelial permeability by tight junctions, *Cell. Mol. Life Sci.* 70 (2013) 631–659.